17th International Particle Accelerator Conference, Deauville, France

Manipulating and diagnosing electron beam with cross-plane coupling in transverse and longitudinal phase spaces

Seongyeol Kim

Pohang Accelerator Laboratory, Republic of Korea

May 20, 2026

Email: sykim12@postech.ac.kr

Contents

- **Motivation of beam manipulation and precise beam diagnostics**
  - For HEP applications and high-bright light sources
  - Generative Phase Space Reconstruction technique (GPSR)
- **4D and 6D beam manipulation + GPSR–based diagnostics**
  - Flat and magnetized beam transformations @ AWA facility
  - Detailed 6D phase space reconstruction @ PAL-XFEL facility
- **Summary and future work**

*e.g., double horn-suppressed, flat slice emittance

Motivation of beam manipulation

Use of magnetized beam:

Reduction of hadron beam emittance: cooling

$$\tau \sim \frac{\rho}{v_{i||} - v_{e||}}$$

Interaction time

ρ: Impact parameter

$v_{i||}$: Longitudinal Ion beam velocity

$v_{e||}$: Longitudinal e-beam velocity

- Y. Sun, Ph.D. Thesis, 2005.
- Y. Derbenev and A. Skrinsky, *Part. Accel.* **8**, 235, 1978.

Use of flat beam:

Direct increases of luminosity

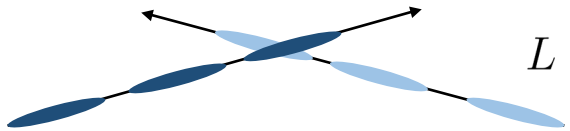

Luminosity

$$L \propto \frac{\eta_{RF} P_{RF}}{E_{cm}^{3/2}} \frac{\sqrt{\delta_{BS}\sigma_z}}{\sigma_y}$$

Small vertical beam size:
by flat beam with large magnetization

$$\epsilon_- \approx \frac{\epsilon_{th}^2}{2\mathcal{L}}$$

- K. Yokoya, P. Chen, Beam-beam phenomena in linear colliders, 2005.
- K. Buesser, Electron-Positron Linear Collider, 2009.

Use of refined electron beam*:

Enhancement of Free Electron Laser quality

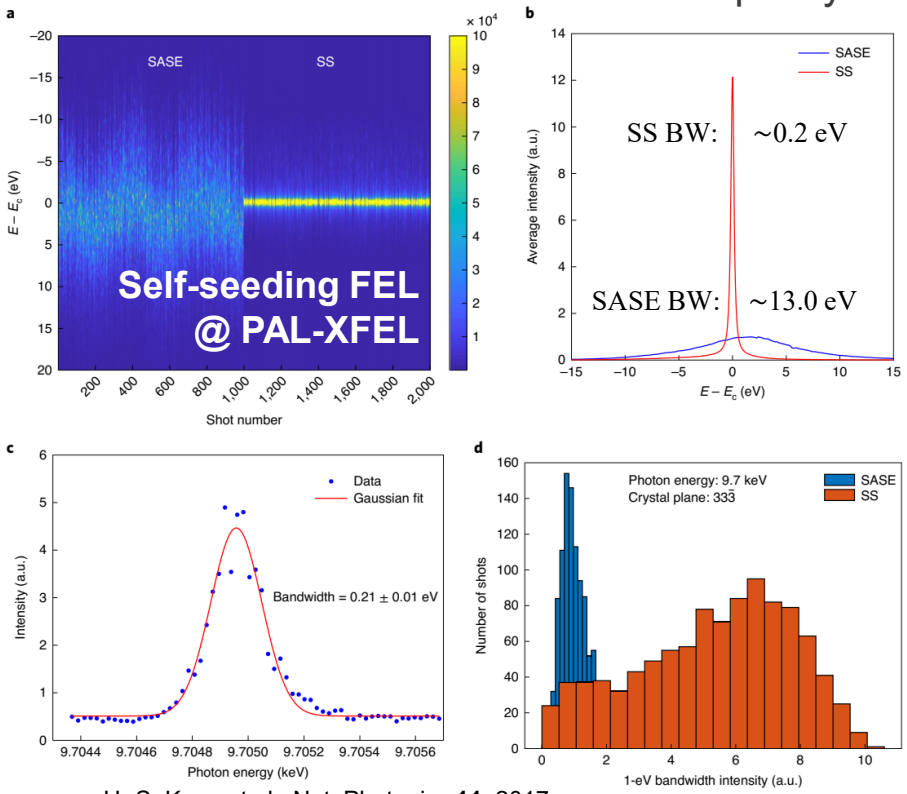

- H.-S. Kang et al., Nat. Photonics **11**, 2017.
- I. Nam *et al., Nat. Photonics* **15**, 2021.

For high-energy physics applications and high-brightness X-ray light:

Proper and accurate beam phase space manipulation is essential

* Accuracy, efficiency, and required time for diagnostics

Beam diagnostics for characterizing manipulated beams

Conventional diagnostics

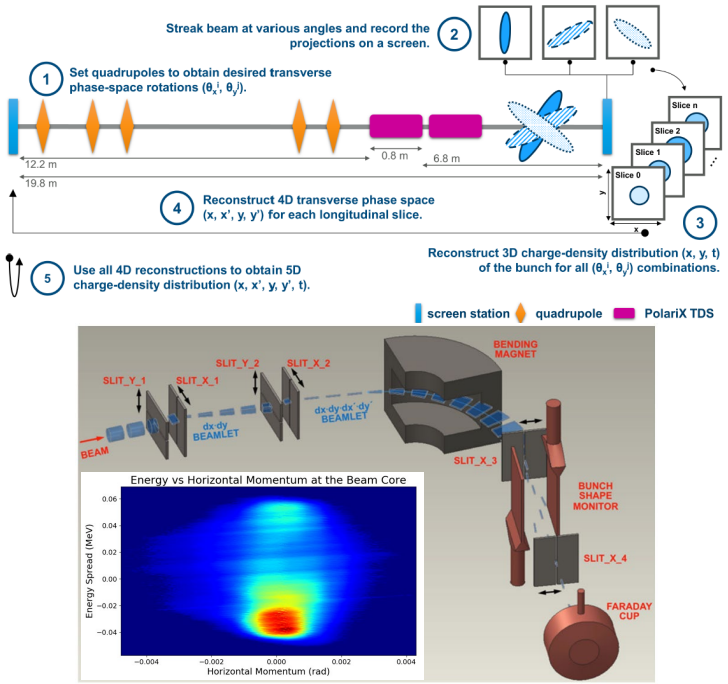

S. Jaster-Merz *et al.*, *PRAB* **27**, 072801, 2024.
B. Cathey *et al.*, *PRL* **121**, 064804, 2018.

Virtual diagnostics

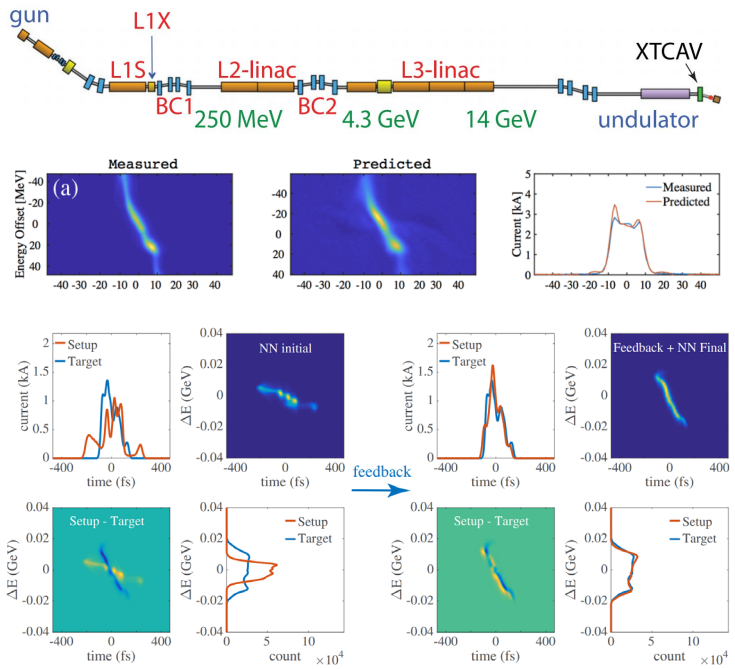

C. Emma *et al.*, *PRAB* **21**, 112802, 2018.
A. Scheinker *et al.*, *PRL* **121**, 044801, 2018.

Generative learnings

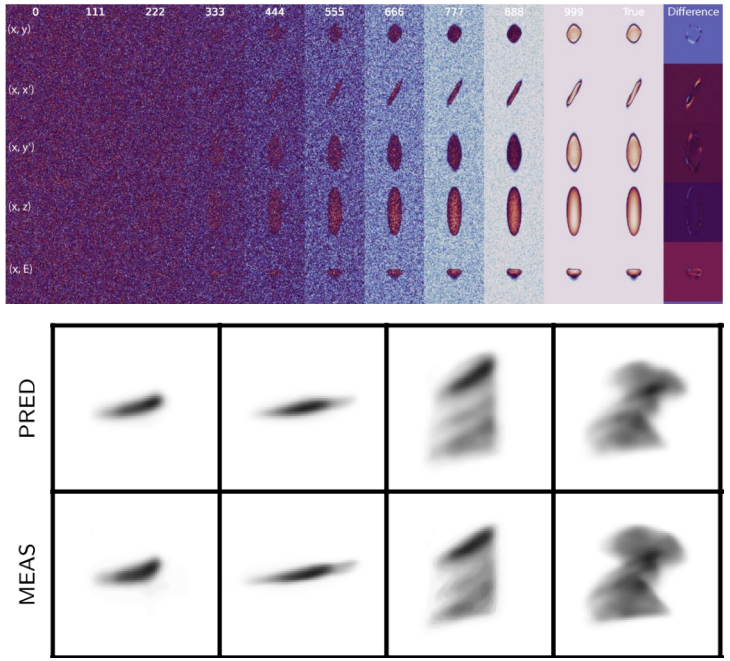

A. Scheinker, *Sci. Rep.* **14**, 29303, 2024.
A. Hoover, *PRAB* **28**, L084601, 2025.

Beam diagnostics from conventional approach to AI/ML technique-incorporated:

allows us to investigate phase space characterization in a robust way*

POHANG ACCELERATOR LABORATORY

- R. Roussel *et al.*, *PRL* **130**, 145001, 2023.
- S. Kim *et al.*, *PRAB* **27**, 074601, 2024.
- R. Roussel *et al.*, *PRAB* **27**, 094601, 2024.
- J.P. Gonzalez-Aguilera *et al.*, *IPAC'24*, 2024.

Generative phase space reconstruction (GPSR)

Based on neural networks and differentiable simulations

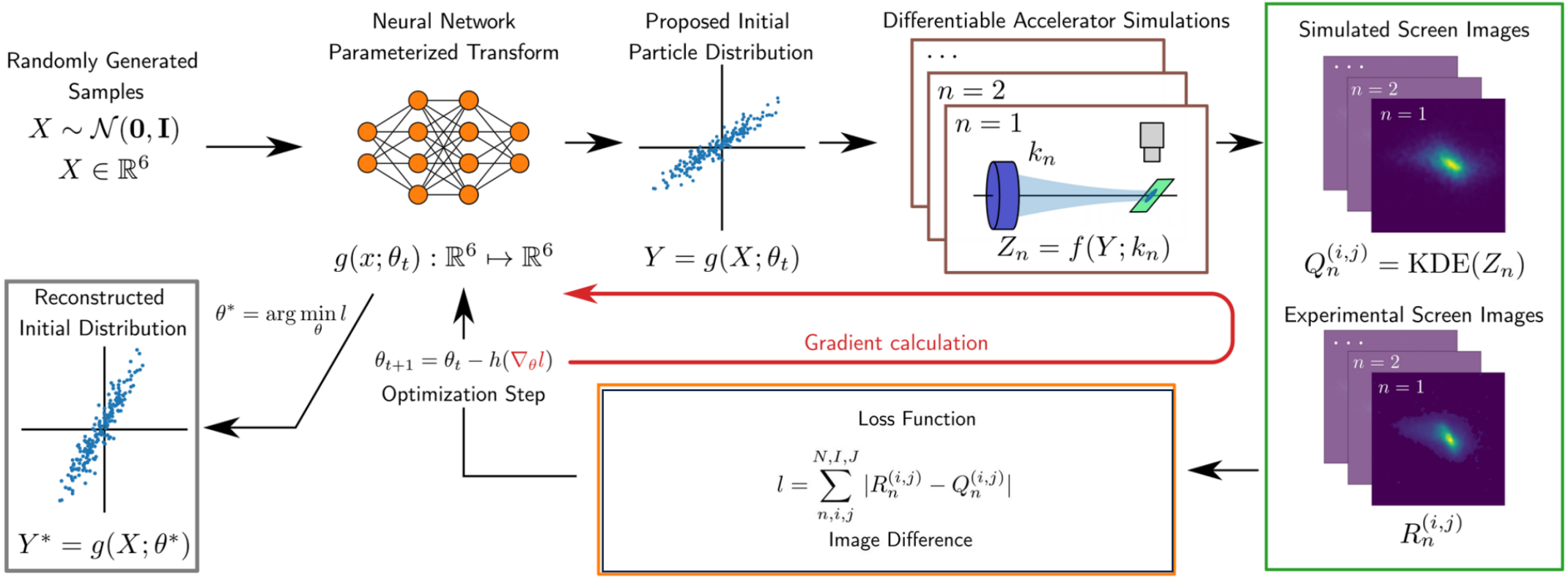

Iteration process to update weights of neural networks:

To reconstruct beam phase space that successfully predicts experimental measurements

4D phase space manipulation and reconstruction

Based on:

- Seongyeol Kim *et al., Phys. Rev. Accel. Beams* **27**, 074601, 2024.
- Seongyeol Kim *et al., Nucl. Inst. Meth. Phys. Res. A* **1072**, 170206, 2025.

What are flat and magnetized beams?

Round beam

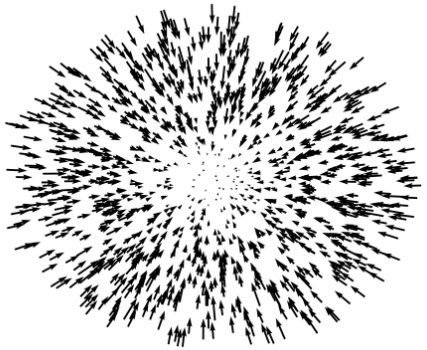

Typical beam we use (does not rotate)

Solenoid field at the cathode

$$\mathbf{P} = \mathbf{p} + e\mathbf{A} = \mathbf{p} + \frac{B_c}{2}(-y\hat{x} + x\hat{y})$$

$$\mathbf{L} = \mathbf{r} \times \mathbf{P}$$

Canonical Angular momentum

Round, magnetized beam

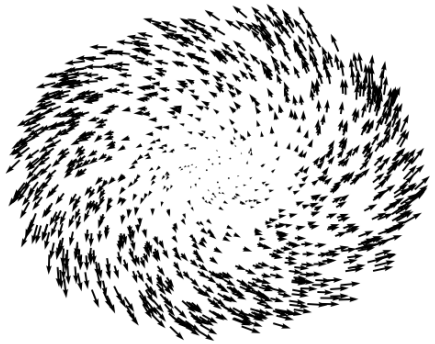

Angular-momentum-dominated beam

$$\Sigma_0 = \begin{bmatrix} \epsilon_{eff} T_0 & \mathcal{L} J \\ -\mathcal{L} J & \epsilon_{eff} T_0 \end{bmatrix}$$

where $T_0 = \begin{bmatrix} \beta & -\alpha \\ \alpha & \gamma \end{bmatrix}$ $J = \begin{bmatrix} 0 & -1 \\ 1 & 0 \end{bmatrix}$

Magnetization

$$\mathcal{L} = \frac{\langle L \rangle}{2 m_e c}$$

Transformation using skew triplet

$$\Sigma_1 = M \Sigma_0 M^{\intercal}$$

$$\Sigma_1 = \begin{bmatrix} \epsilon_+ T_+ & 0 \\ 0 & \epsilon_- T_- \end{bmatrix}$$

Flat beam

Eigenemittance

$$\epsilon_+ \approx 2\mathcal{L} \quad \epsilon_- \approx \frac{\epsilon_{th}^2}{2\mathcal{L}}$$

ϵ_{th} Uncorrelated emittance

For magnetization = 50 um, and ϵ_{th}= 5.0 um,

ϵ_+ (Emit_nx) (mm mrad)	ϵ_- (Emit_ny) (mm mrad)
100	0.25

*Relativistic factor larger than 50

Back-to-back beam transformations @ AWA facility

Back-to-back(B2B): Round-to-flat and flat-to-round(magnetized) beam transformations*

Motivation of beam transformations:

- Difficulty of high-energy* magnetized beam transport: make it easy by decoupling
- Then, transformation back to magnetized condition at the application section (e.g., cooling)

High-energy magnetized beam generation using photoinjector → Flat beam transformation + beam transport → Magnetized beam transformation + application

Goal of demonstration:

- Experimental demo of back-to-back transformations at Argonne Wakefield Accelerator (AWA) Facility

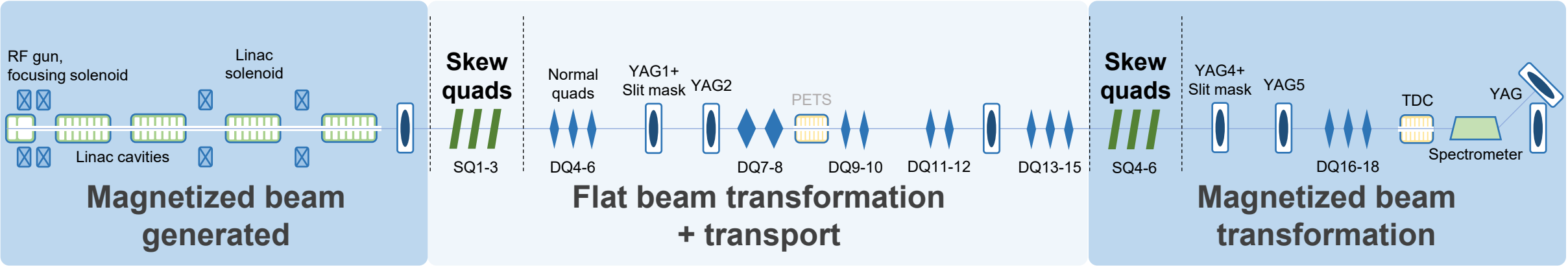

Experimental demonstration of beam transformations

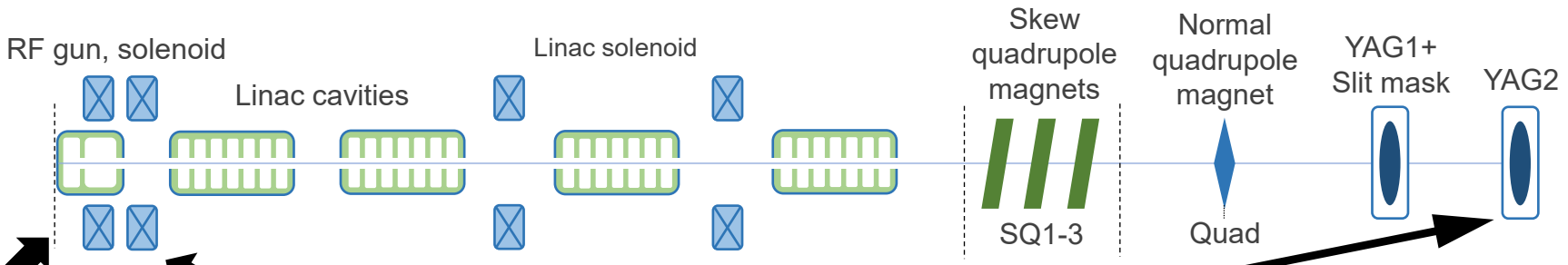

Use of multi-lens array (MLA)

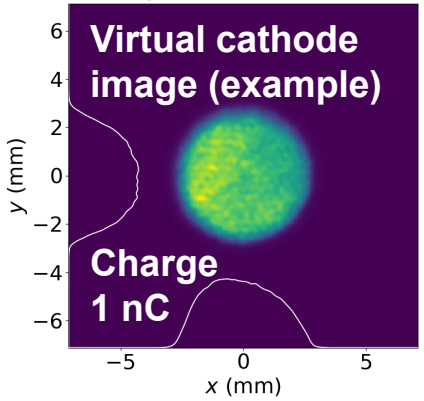

No bucking solenoid: Non-zero B-field at cathode

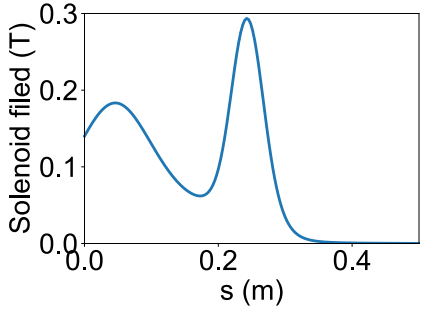

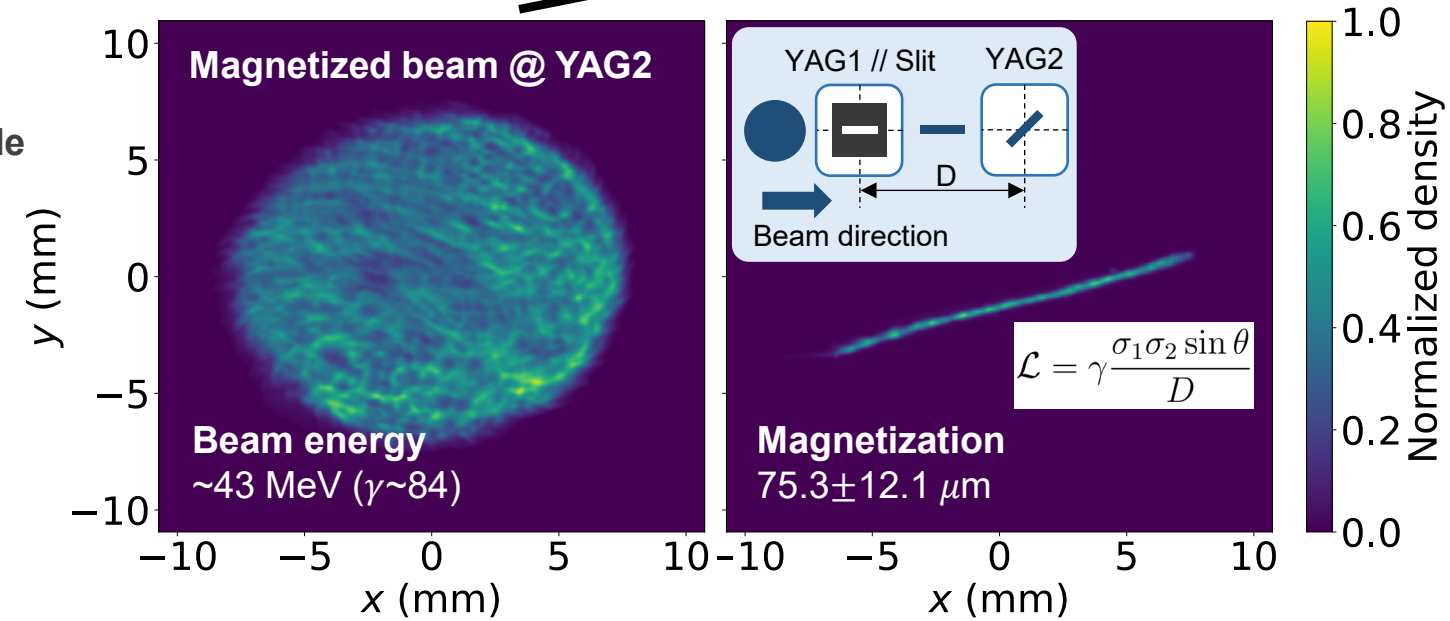

Experimental demonstration of beam transformations

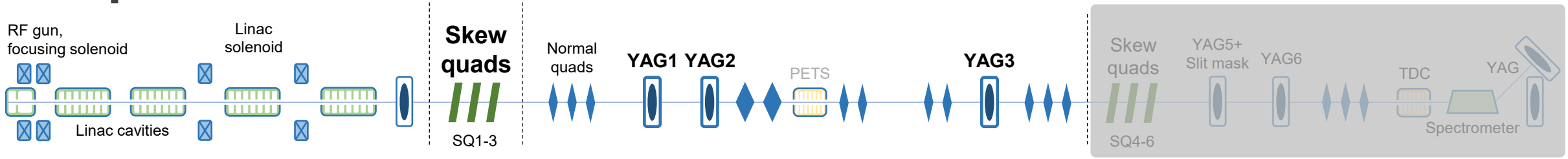

For magnetized beam: $\mathbf{Y} = C\mathbf{X}$

$$\mathbf{X} = (x, p_x), \mathbf{Y} = (y, p_y)$$

Twiss Parameters

$$C = \frac{\mathcal{L}}{\epsilon_{eff}} \begin{bmatrix} \alpha & \beta \\ -\frac{1+\alpha^2}{\beta^2} & -\alpha \end{bmatrix}$$

where $\epsilon_{eff} = \sqrt{\epsilon_{th}^2 + \mathcal{L}^2}$

RFBT matrix calculation

$$\begin{pmatrix} \mathbf{X} \\ \mathbf{Y} \end{pmatrix} = \frac{1}{2} \begin{pmatrix} [A + B + (A - B)C]\mathbf{X} \\ [A - B + (A + B)C]\mathbf{X} \end{pmatrix}$$

where skew triplet matrix,

$$M_{SQ} = \begin{pmatrix} A+B & A-B \\ A-B & A+B \end{pmatrix}$$

RFBT goal: find skew quad settings that vanishes $\mathbf{Y}$

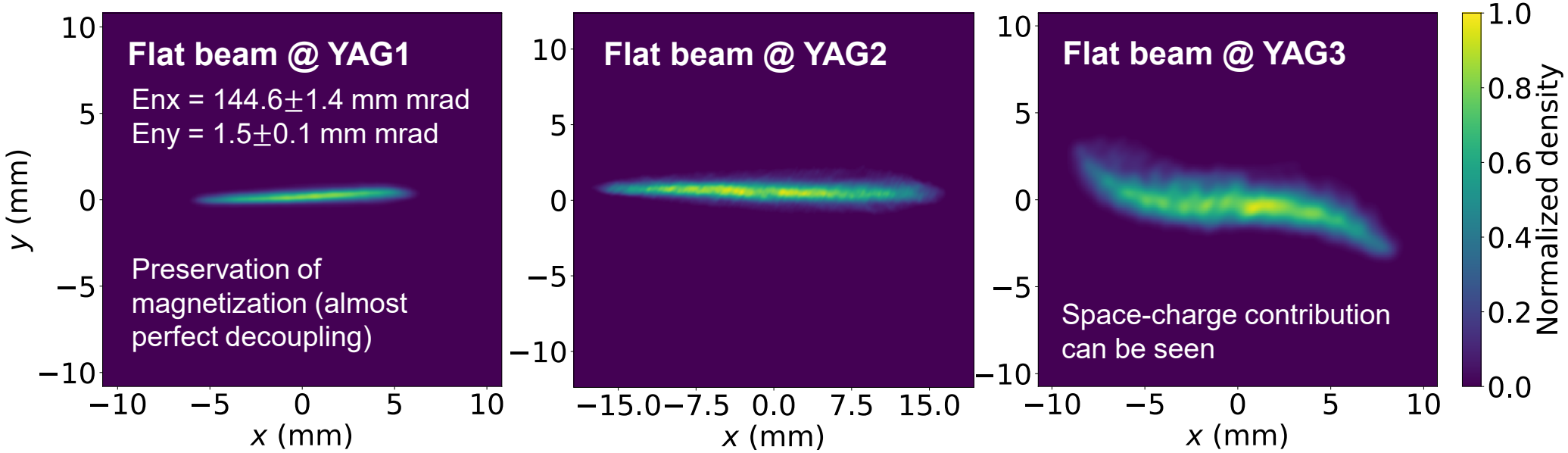

Experimental demonstration of beam transformations

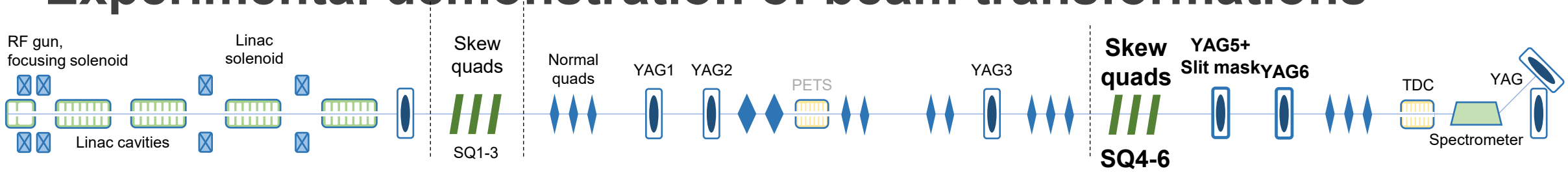

Flat to round beam transformation (simulations with different quad signs)

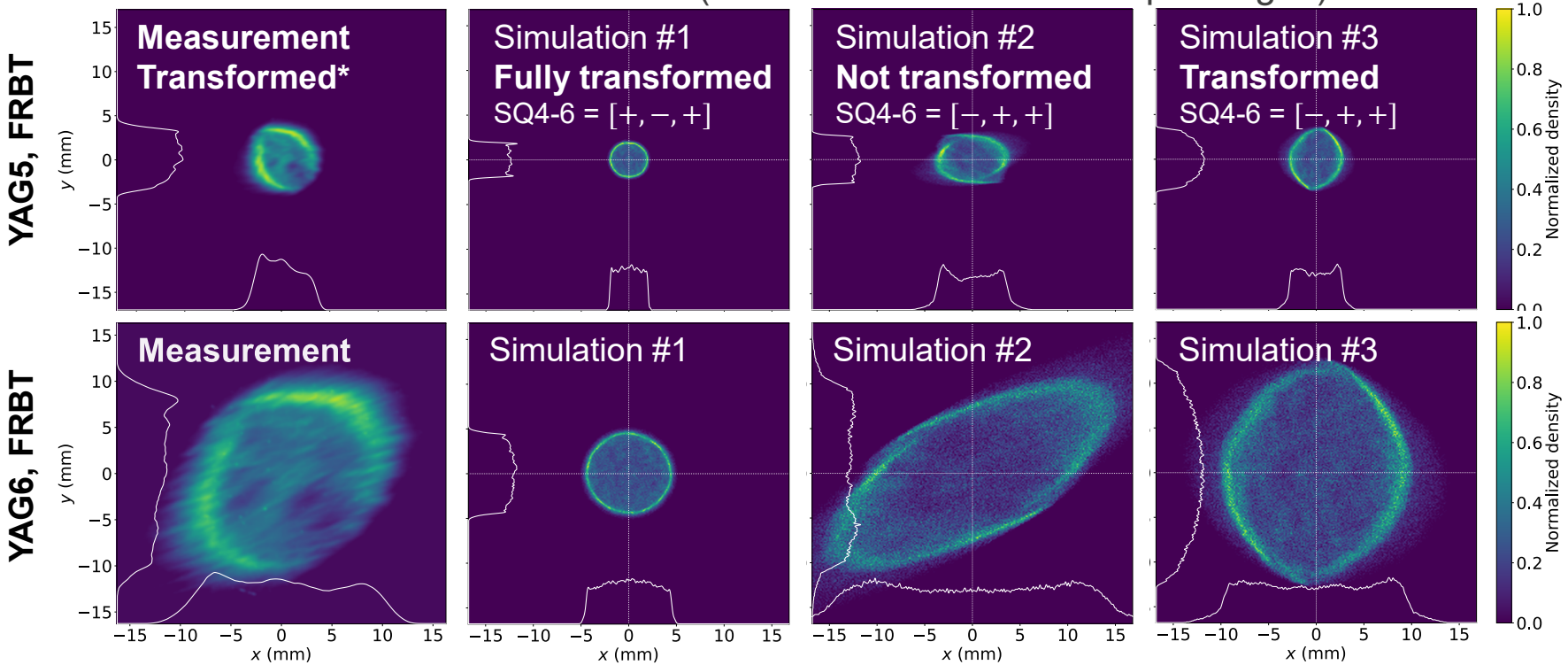

Magnetization
(slit-measurement)
74.3±17.7 μm

Magnetization
74.1 μm

Magnetization
68.8 μm

Magnetization
71.9 μm

*For simulation #2,

$$|\gamma\langle xy'\rangle| \neq |\gamma\langle x'y\rangle|$$

Thus, not transformed

precise beam diagnostic method is required for accurate validation of transversely coupled beam!

GPSR technique

Characterization of magnetized beam using GPSR

Different UV distribution and solenoid field were applied in this case

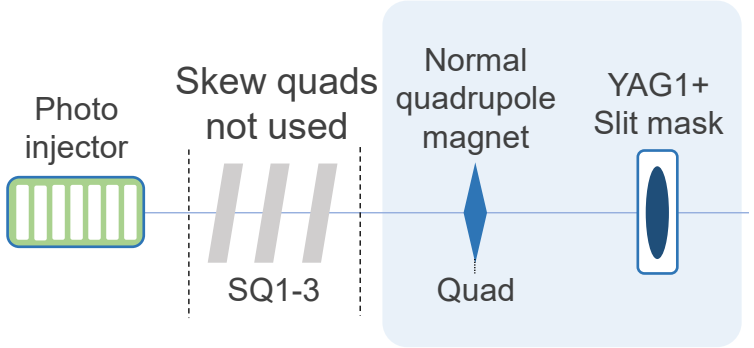

GPSR setup:

- 21 quadscan samples (half for train)
- 250x250 image bins
- 100k particles, 4000 epochs

measurement Test dataset

Comparison of training / test dataset (images @ YAG1)

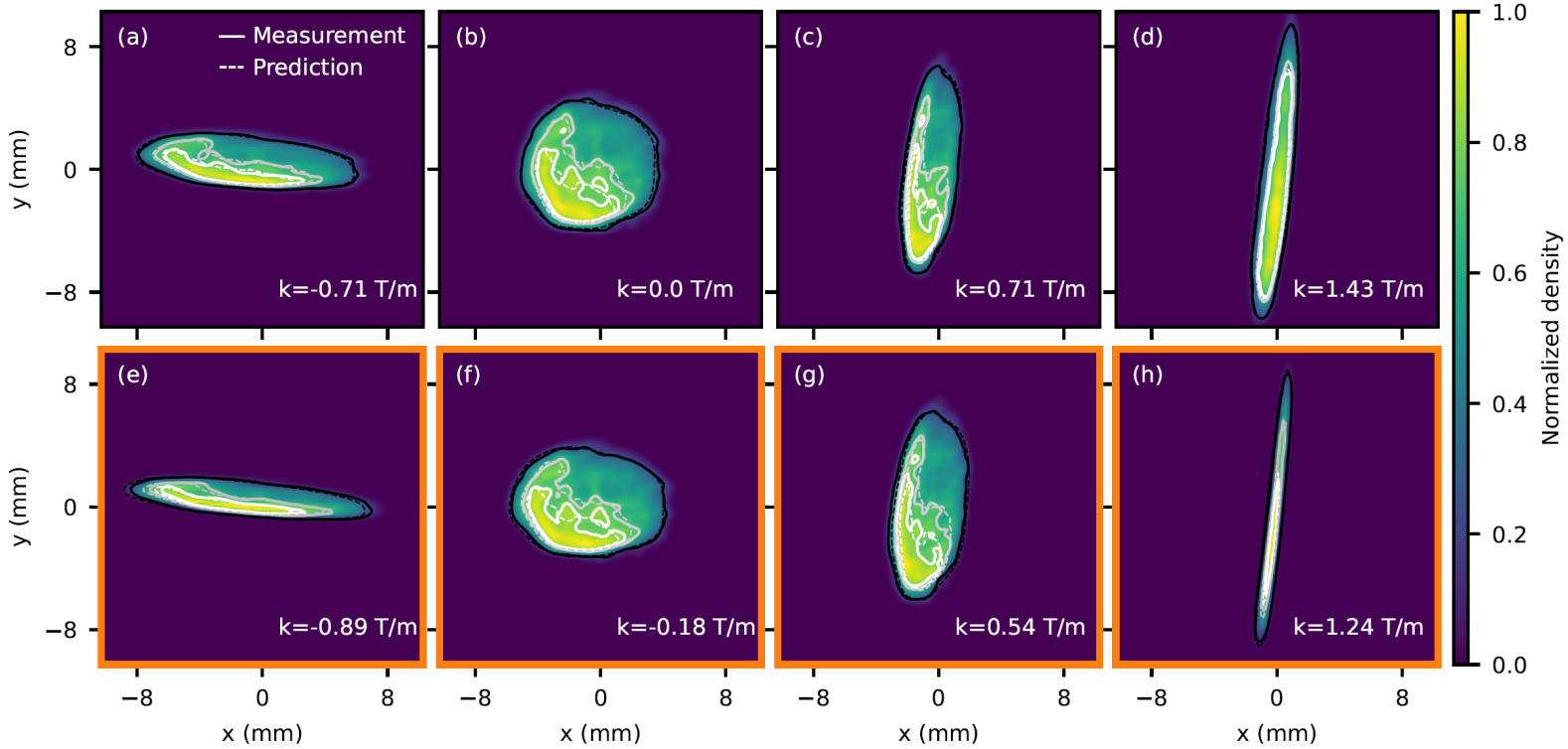

Characterization of magnetized beam using GPSR

Different UV distribution and solenoid field were applied in this case

Magnetized beam matrix

$$\begin{bmatrix} \epsilon_{eff}\beta_x & -\epsilon_{eff}\alpha_x & 0 & \boxed{\mathcal{L}} \\ -\epsilon_{eff}\alpha_x & \epsilon_{eff}\gamma_x & -\mathcal{L} & 0 \\ 0 & \boxed{-\mathcal{L}} & \epsilon_{eff}\beta_y & -\epsilon_{eff}\alpha_y \\ \mathcal{L} & 0 & -\epsilon_{eff}\alpha_y & \epsilon_{eff}\gamma_y \end{bmatrix} \Rightarrow \left|\gamma\left(\langle xy'\rangle - \langle yx'\rangle\right)\right|/2$$

$$\epsilon_{eff} = \sqrt{\epsilon_{th}^2 + \mathcal{L}^2}$$

β, α, γ: Twiss parameters

Magnetization, case	Value (um)
Reconstruction	**44.0**
Slit measurement	**47.2±0.9**

GPSR for magnetized beams:

Successful to obtain detailed phase space information including couplings

Reconstructed phase space

(unit: mm / mrad)

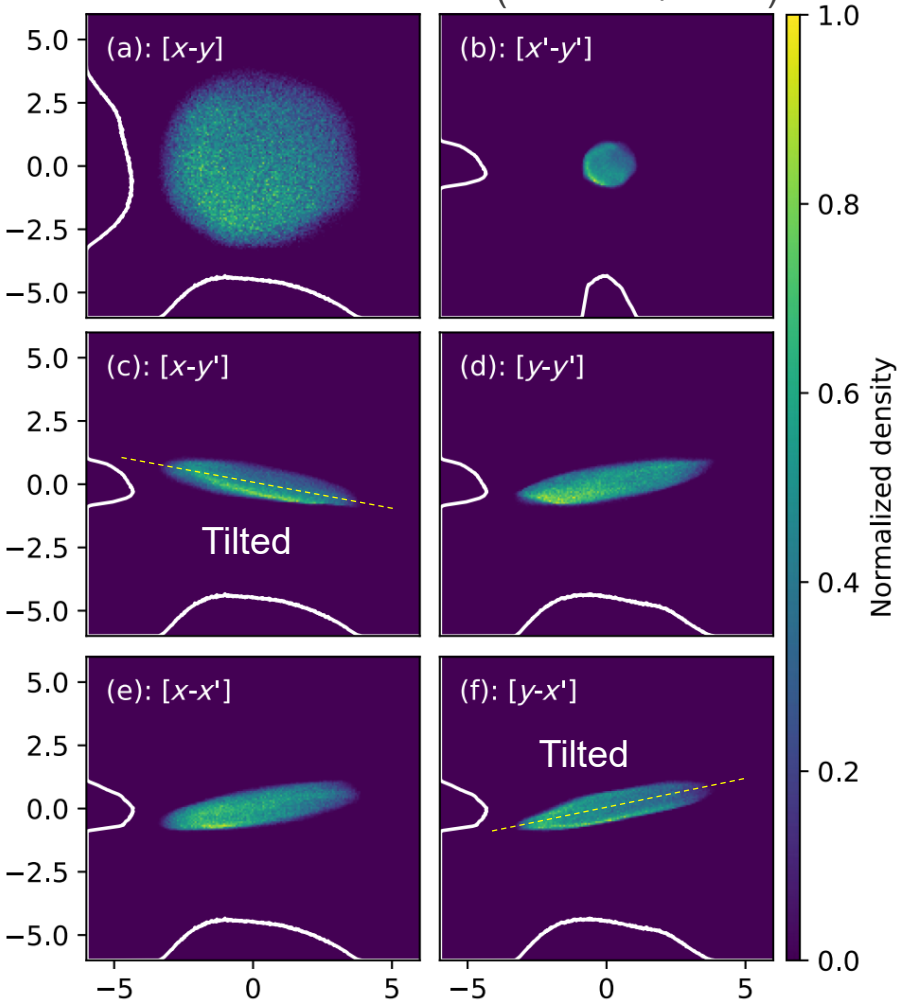

Characterization of flat beam using GPSR

Different UV distribution and solenoid field were applied (also compared to magnetized beam GPSR)

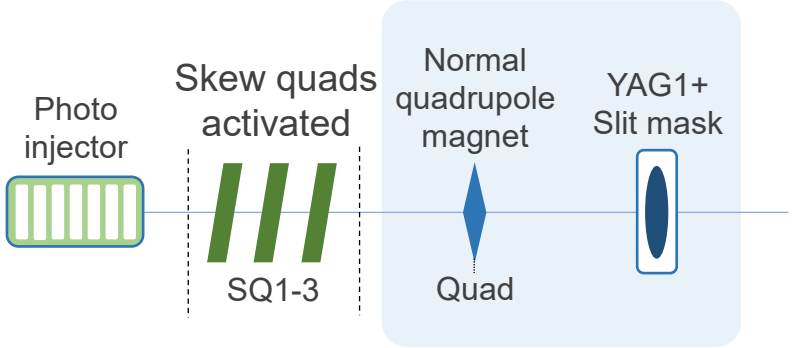

GPSR setup:

- 21 quadscan samples (half for train)
- 100k particles, 4000 epochs

measurement Test dataset

Comparison of training / test dataset (images @ YAG1)

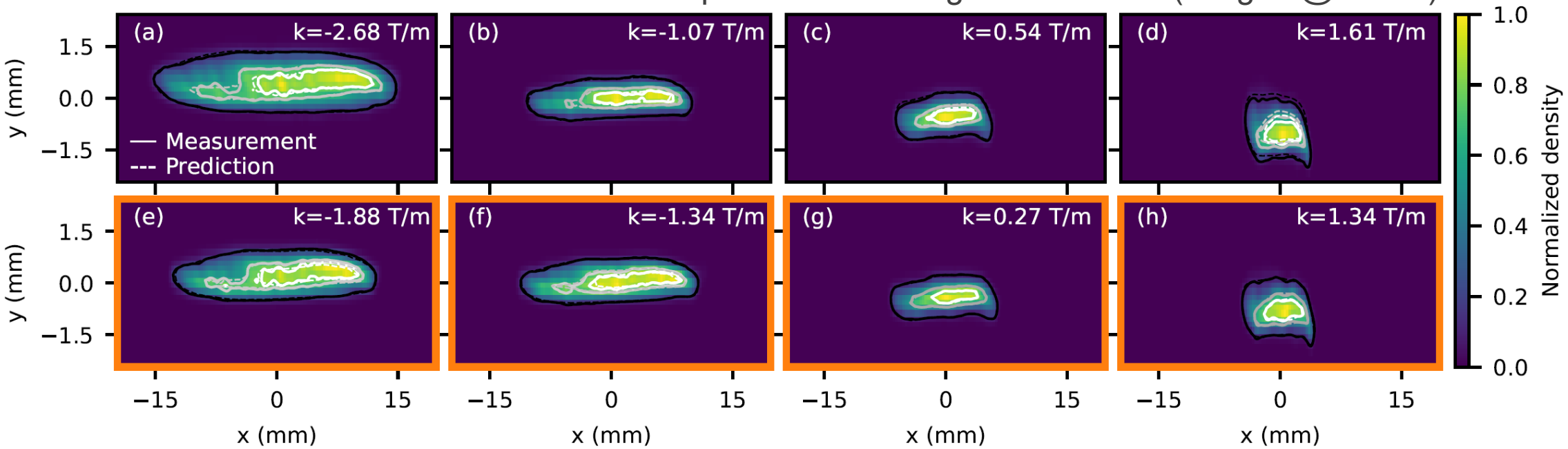

Characterization of flat beam using GPSR

Different UV distribution and solenoid field were applied (also compared to magnetized beam GPSR)

After beam transformation, beam covariance becomes:

$$\begin{bmatrix} \langle x^2\rangle & \langle xx'\rangle & \langle xy\rangle & \langle xy'\rangle \\ \langle xx'\rangle & \langle x'^2\rangle & \langle yx'\rangle & \langle x'y'\rangle \\ \langle xy\rangle & \langle xy'\rangle & \langle y^2\rangle & \langle yy'\rangle \\ \langle yx'\rangle & \langle x'y'\rangle & \langle yy'\rangle & \langle y'^2\rangle \end{bmatrix} = \begin{bmatrix} \epsilon_+\beta_+ & -\epsilon_+\alpha_+ & 0 & 0 \\ \epsilon_+\alpha_+ & \epsilon_+\gamma_+ & 0 & 0 \\ 0 & 0 & \epsilon_-\beta_- & -\epsilon_-\alpha_- \\ 0 & 0 & \epsilon_-\alpha_- & \epsilon_-\gamma_- \end{bmatrix}$$

Where eigen-emittances: $\epsilon_+ \approx 2\mathcal{L} \quad \epsilon_- \approx \frac{\epsilon_{th}^2}{2\mathcal{L}}$

ϵ_{th} Uncorrelated emittance

Case	Emit_nx (ε_+) (mm mrad)	Emit_ny (ε_-) (mm mrad)
Reconstruction	**140.14**	**1.53**
Measurement (Quadrupole scan)	**144.64±1.36**	**1.47±0.10**

Also, GPSR technique successfully reconstructed flat beams!

Reconstructed phase space

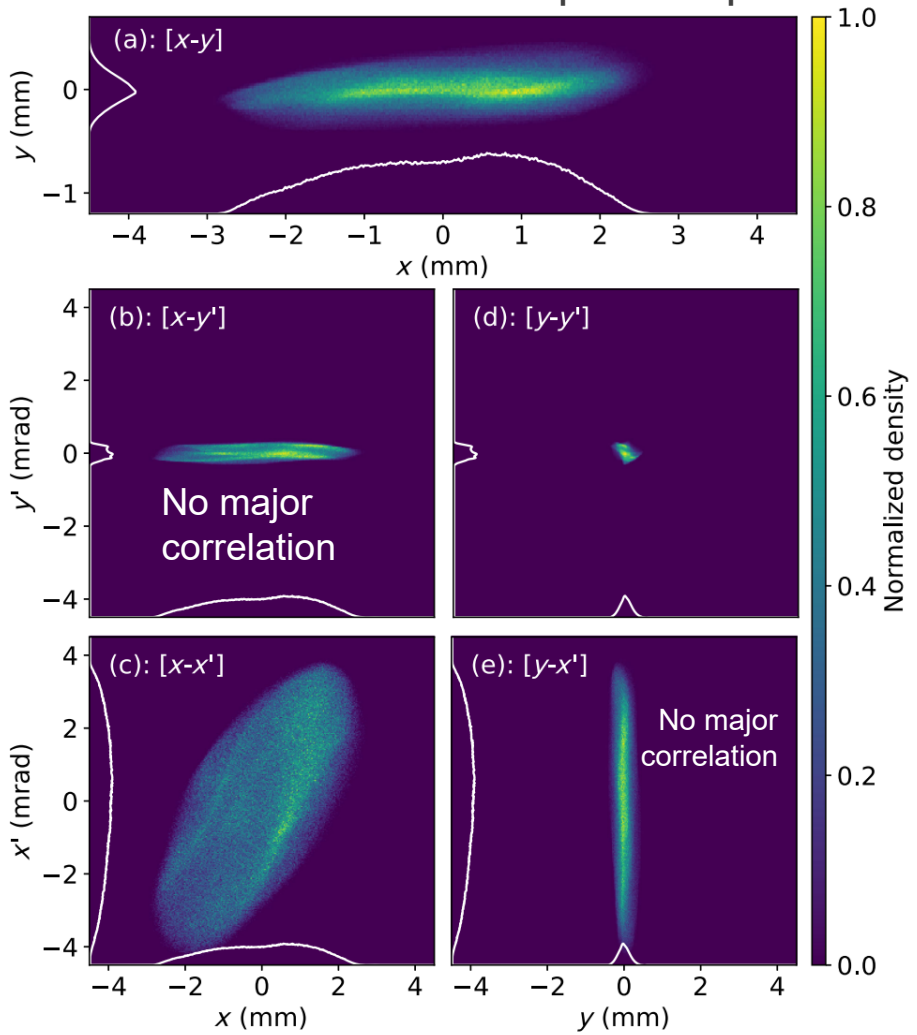

6D phase space manipulation and reconstruction

Based on:

- Seongyeol Kim *et al., Sci. Rep.* **15**, 43049, 2025.

Pohang Accelerator Laboratory, X-ray Free Electron Laser

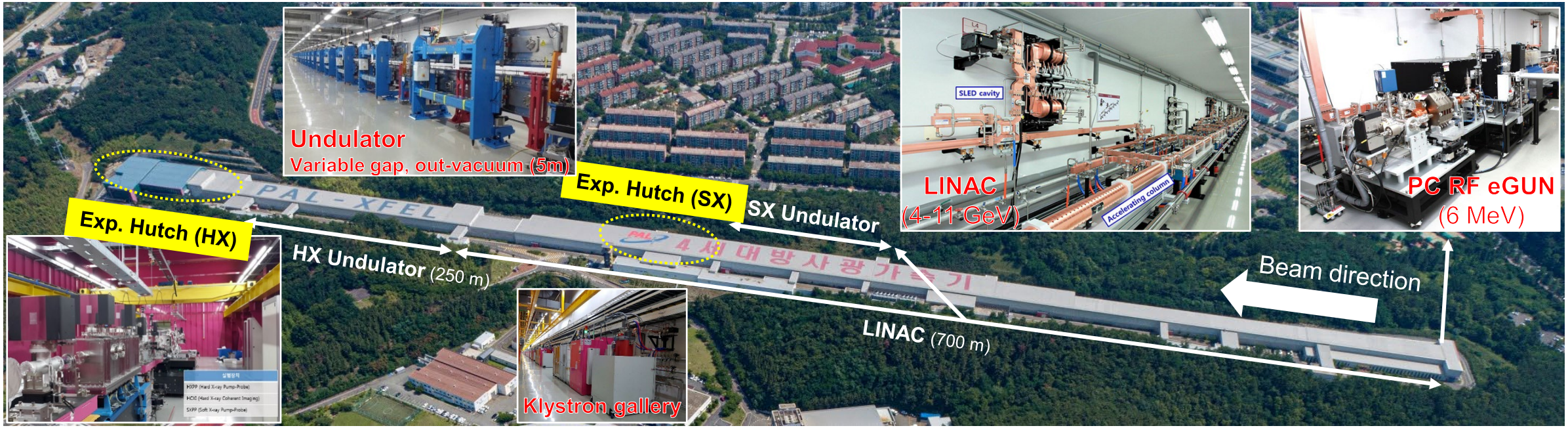

PAL-XFEL Layout

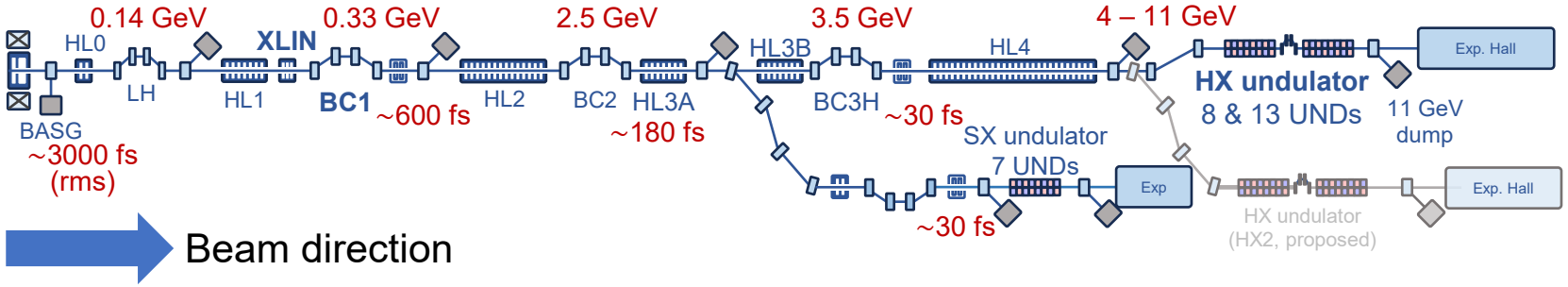

Undulator Line	HX	SX
Photon energy (keV)	2.0~20.0	0.25~1.25
Beam energy (GeV)	4~11	3.0
Beam charge (pC)	190/250	160/250
Peak current (kA)	~3	~2.5
E_{ph} tuning	Energy/Gap	Gap
Repetition rate (Hz)	60	60
FEL intensity	> 1 mJ	> 250 μJ

Beam manipulation @ PAL-XFEL HX

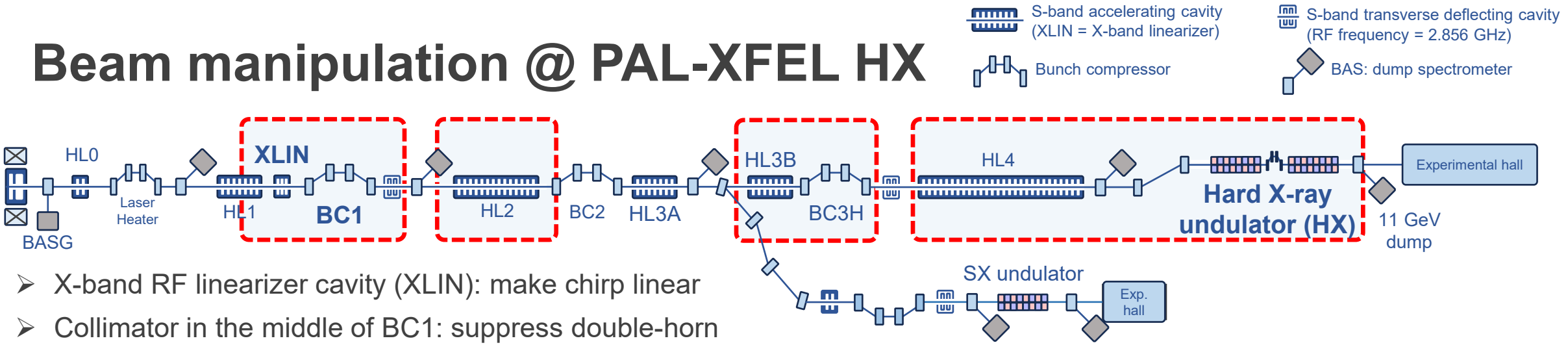

- X-band RF linearizer cavity (XLIN): make chirp linear
- Collimator in the middle of BC1: suppress double-horn
- BC3H: emittance optimization against CSR
- HL2, HL4, HX sections: FODO lattice matching

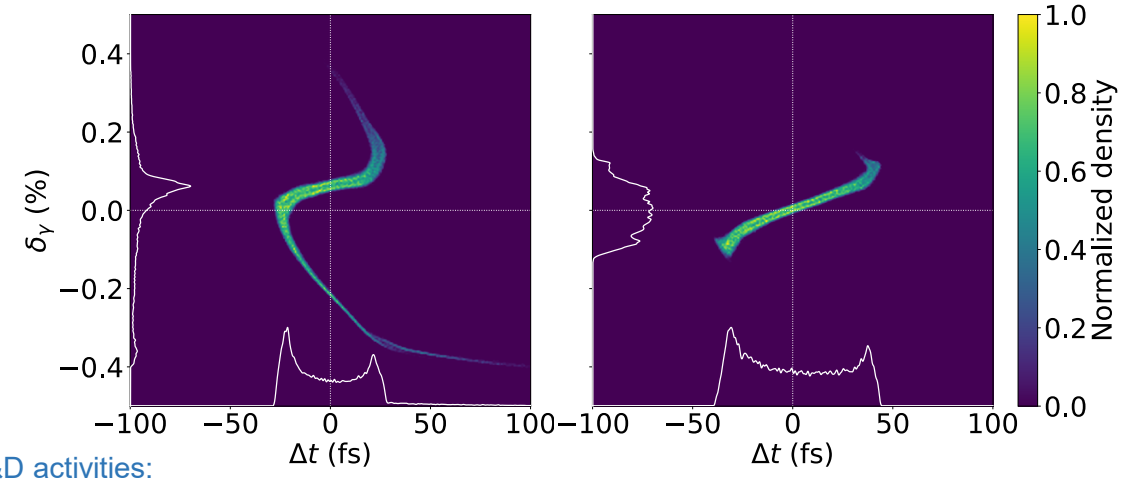

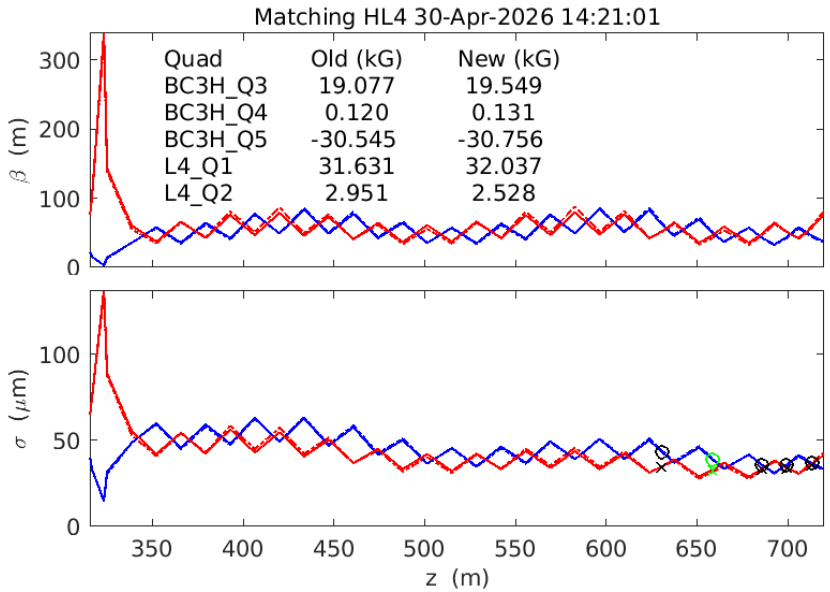

Other R&D activities:

- UV laser control: **Seong-Hoon Kwon *et al.*, TUP7721 (Tuesday poster)**
- FEL mode development: **Chi Hyun Shim *et al.*, TUP2662 (Tuesday poster)**
- Beam phase space diagnostics: **Myunghoon Cho *et al.*, MOP6656 (Monday poster)**

- R. Roussel *et al.*, *PRAB* **27**, 094601, 2024.
- J.P. Gonzalez-Aguilera *et al.*, *IPAC'24*, 2024.
- *R. Roussel *et al.*, arXiv:2604.20125, 2026.

6D GPSR using transverse deflecting cavity

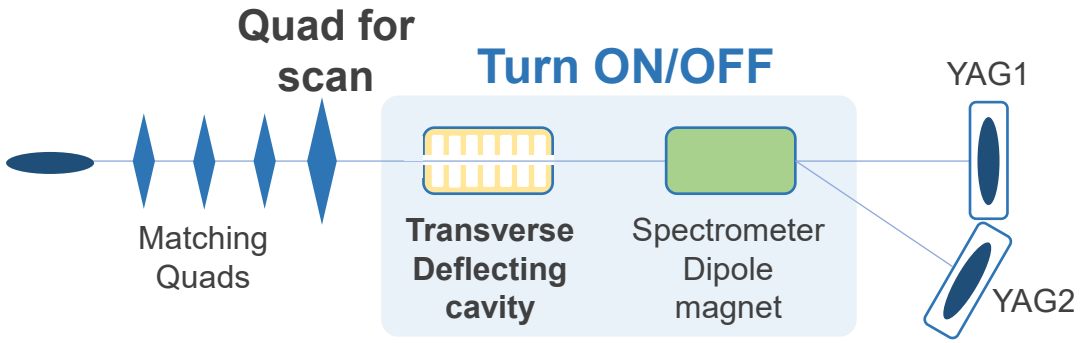

CSR characterization

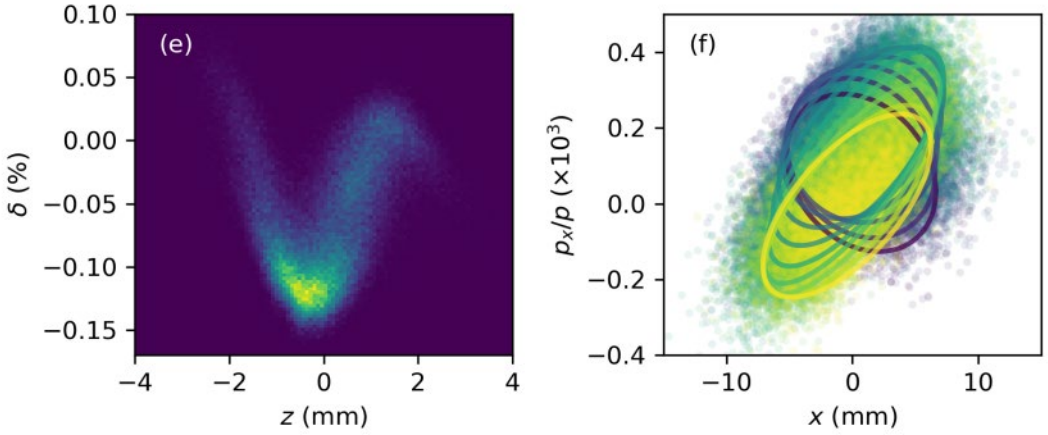

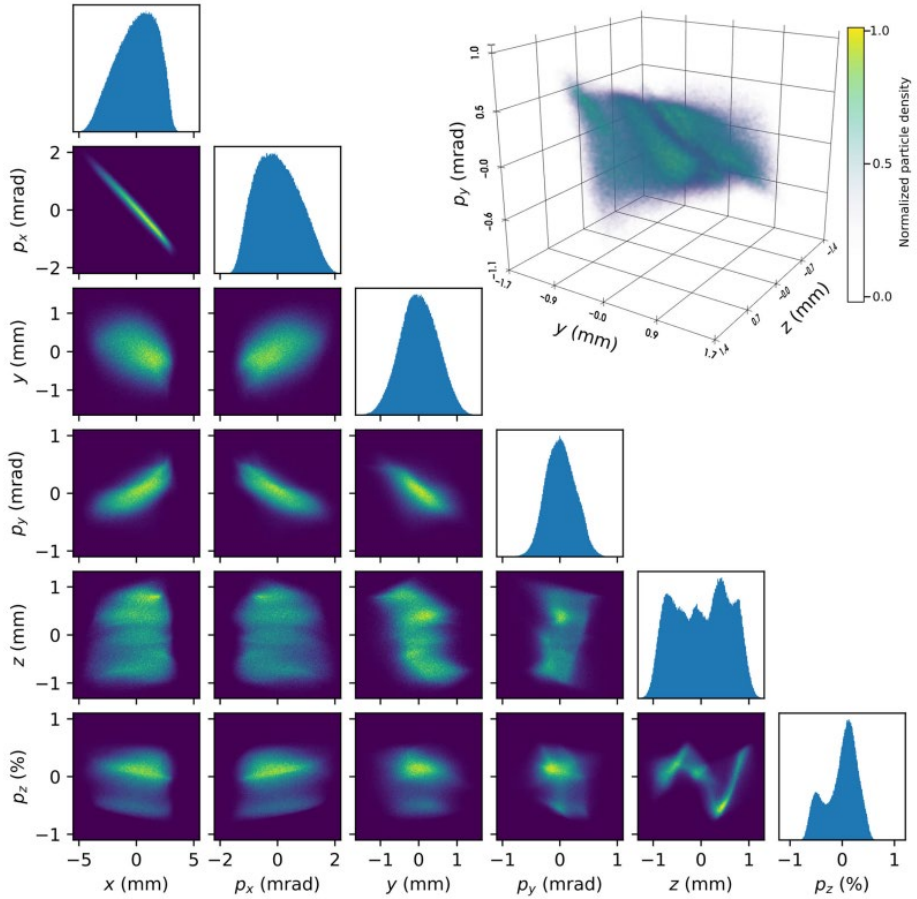

➡ 6-dimensional phase space reconstruction is also successfully performed and currently deployed @ LCLS-II, SLAC*

POHANG ACCELERATOR LABORATORY

6D GPSR using RF accelerating cavity

Inspired by conventional longitudinal emittance measurement*

*Longitudinal emittance:
- D. Dowell *et al., In. Proc. PAC'03,* 2003.
- D. Dowell *et al., Nucl. Inst. Meth. Phys. Res. A* **507**, 331, 2003.

Longitudinal phase space tomography:
- H. Loos *et al., Nucl. Inst. Meth. Phys. Res. A* **528**, 189-193, 2004.

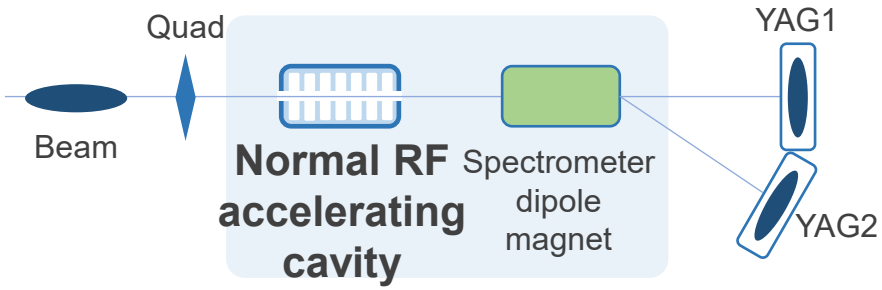

$$\Delta E(z) = eV\cos\left(k_{RF}z + \phi_{RF}\right)$$

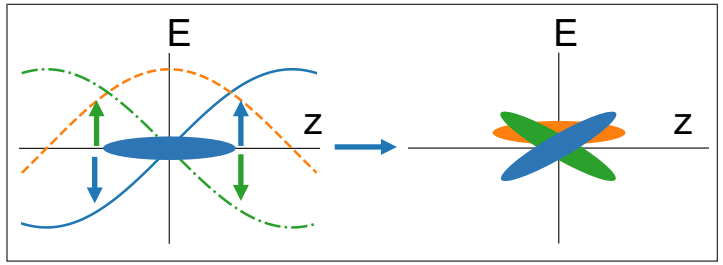

For a given longitudinal distribution:

➡ **Energy changes induced by the cavity can be captured at the spectrometer screen**

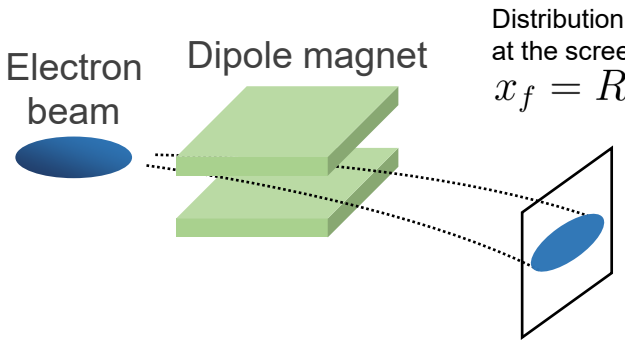

Distribution at the screen

$$x_f = R_{11}x_0 + R_{12}x_0' + R_{16}\,\delta_0$$

Dispersion of dipole magnet

Fractional energy spread $\delta = \dfrac{\Delta E}{E_{ref}}$

Top: longitudinal phase space **Bottom: beam at spectrometer screen**

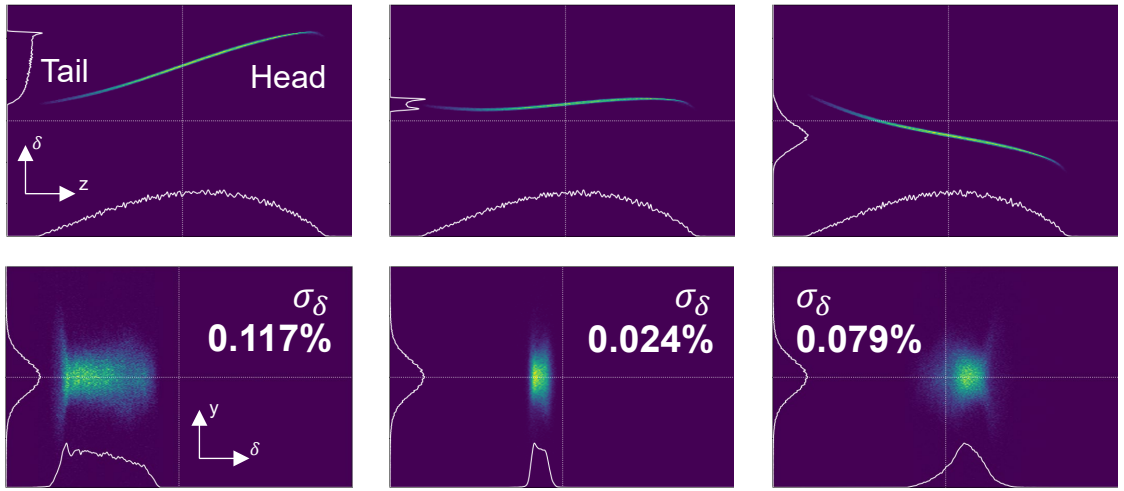

POHANG ACCELERATOR LABORATORY

6D GPSR using RF accelerating cavity

Inspired by conventional longitudinal emittance measurement*

***Longitudinal emittance:**
- D. Dowell *et al., In. Proc. PAC'03,* 2003.
- D. Dowell *et al., Nucl. Inst. Meth. Phys. Res. A* **507**, 331, 2003.

Longitudinal phase space tomography:
- H. Loos *et al., Nucl. Inst. Meth. Phys. Res. A* **528**, 189-193, 2004.

Transfer matrix for cavity and drift

$$M = \begin{pmatrix} 1 & l \\ 0 & 1 \end{pmatrix} \begin{pmatrix} 1 & 0 \\ -V\sin(\phi_{RF}) & 1 \end{pmatrix} \quad \text{where} \quad \Sigma_i = \begin{pmatrix} \sigma_{11} & \sigma_{12} \\ \sigma_{21} & \sigma_{22} \end{pmatrix} = \begin{pmatrix} <z^2> & <z\delta> \\ <z\delta> & <\delta^2> \end{pmatrix}$$

$$\sigma_{22}^{YAG} = \sigma_\delta^2 = V^2\sigma_{11}\phi^2 - 2V\sigma_{12}\phi + \sigma_{22}$$

RMS energy spread at the screen $= A\phi^2 + B\phi + C$ ➡ Similar to normal quadscan: Estimation of second-order moments

$$\epsilon_z = \sqrt{\sigma_{11}\sigma_{12} - \sigma_{12}^2}$$ ➡ **Emittance**

Example: Quadratic behavior of energy spread

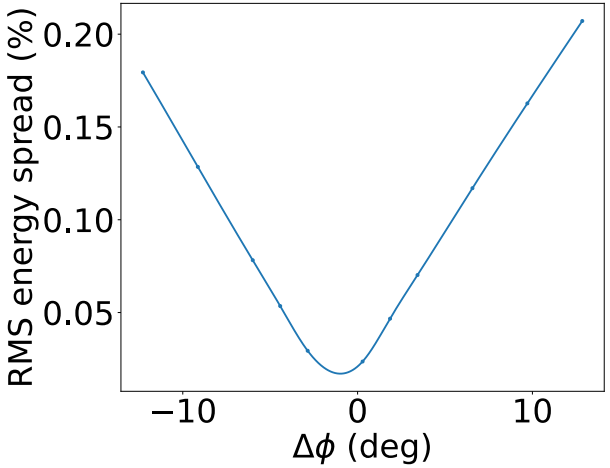

By combining quadrupole field and cavity phase scans, **and GPSR**:

We can obtain complete 6-dimensional coupled phase space of the beam

Experimental setup for the GPSR @ PAL-XFEL

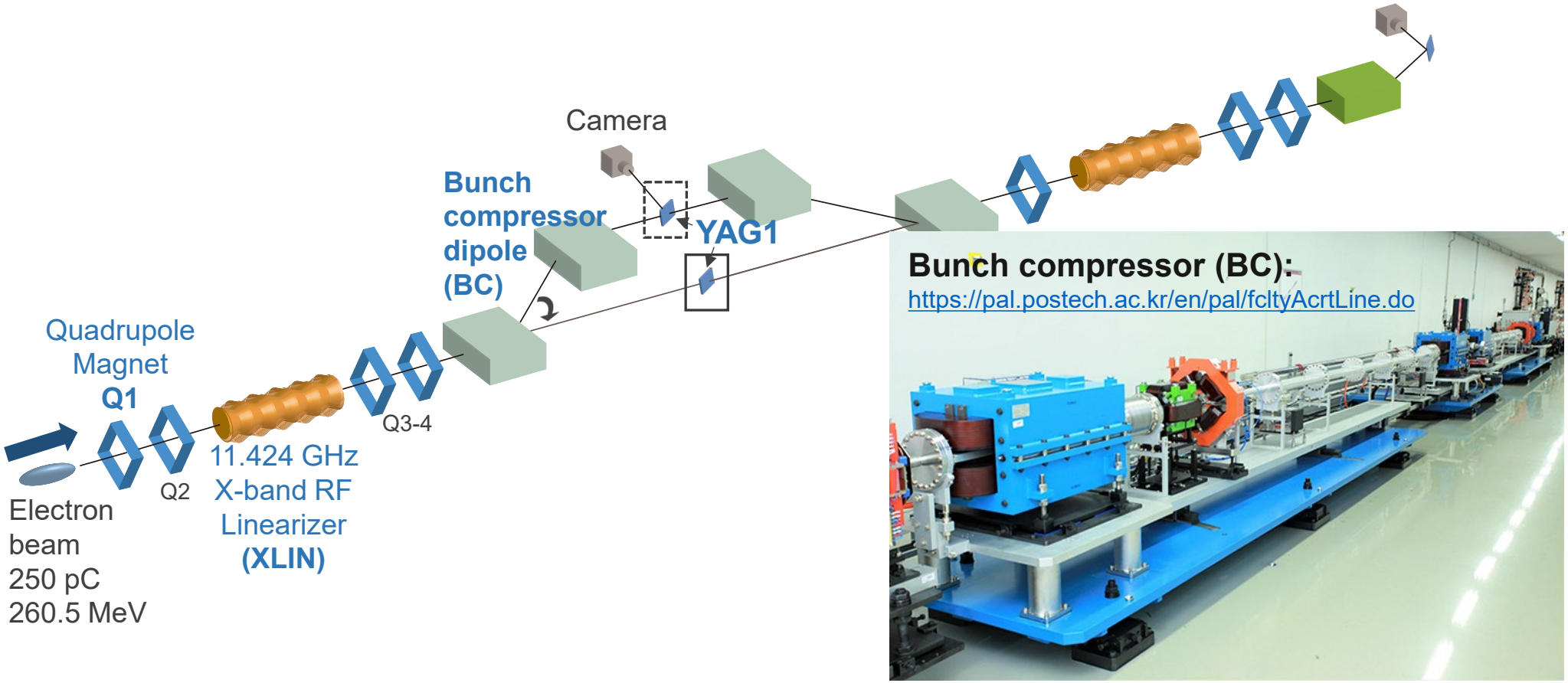

Experimental setup for the GPSR @ PAL-XFEL

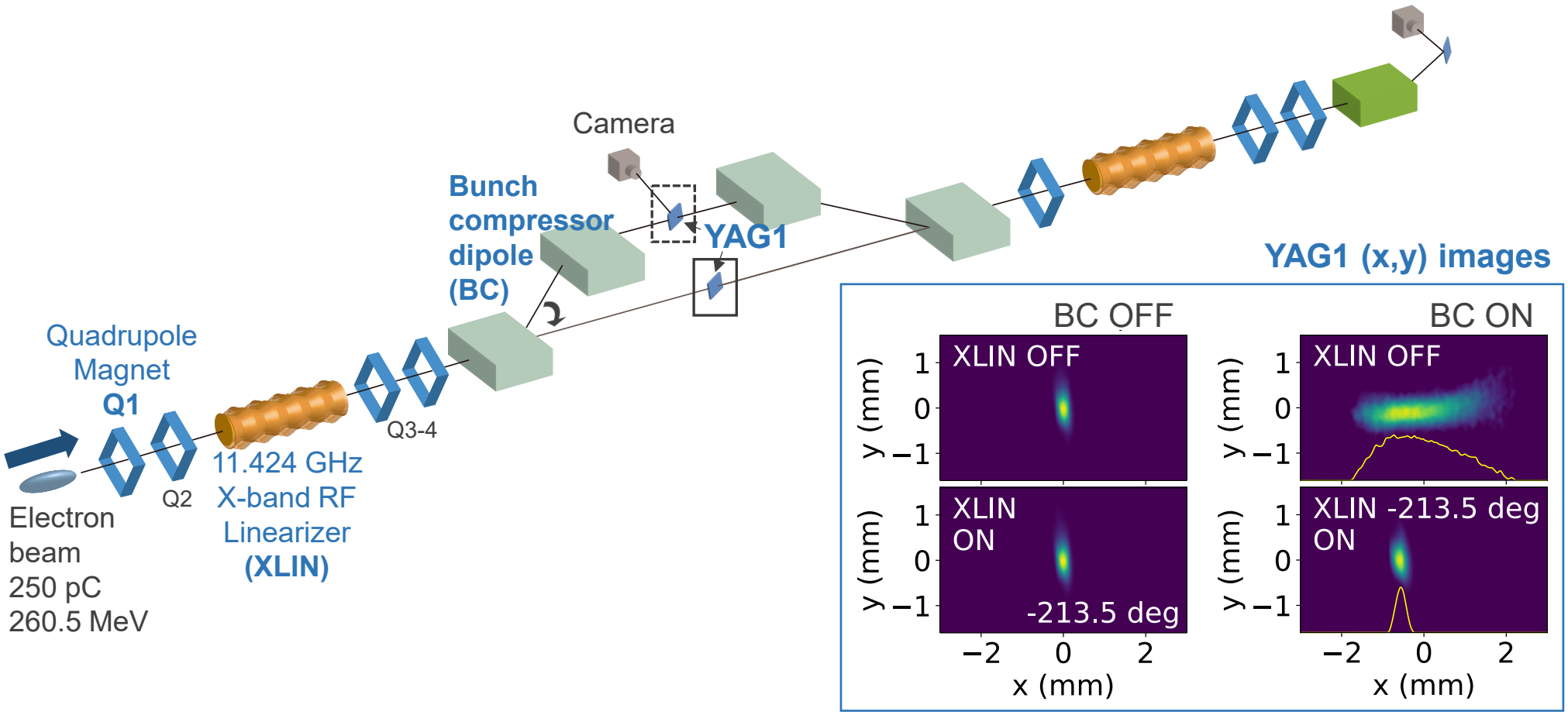

- Bmad-X: https://github.com/bmad-sim/Bmad-X
- Transition in progress from Bmad-X to Cheetah simulation @ PAL-XFEL: https://github.com/desy-ml/cheetah

Experimental setup for the GPSR @ PAL-XFEL

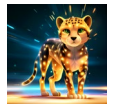

GPSR demo section

Parameters	# of samples
Quad strength	16
XLIN phase	5
BC condition	2
Total samples	160(80 for train)

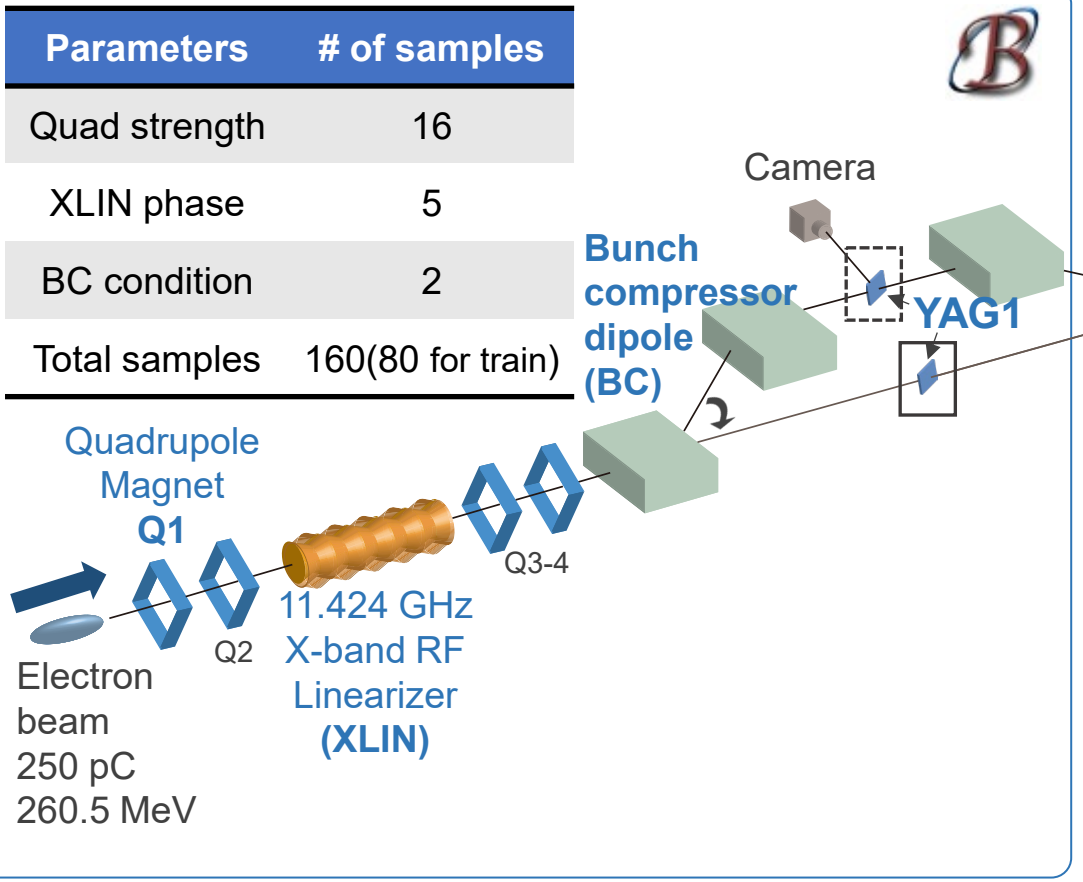

GPSR validation section

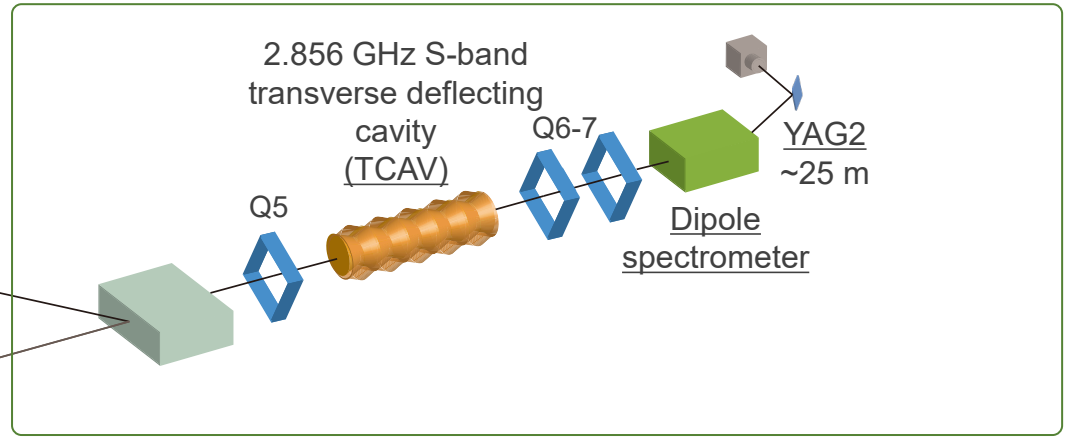

GPSR setup	Values
# of particles	100,000
# of iterations	1,000
Training time	~30 mins (Nvidia A100)

Comparison of training and test datasets @ YAG1

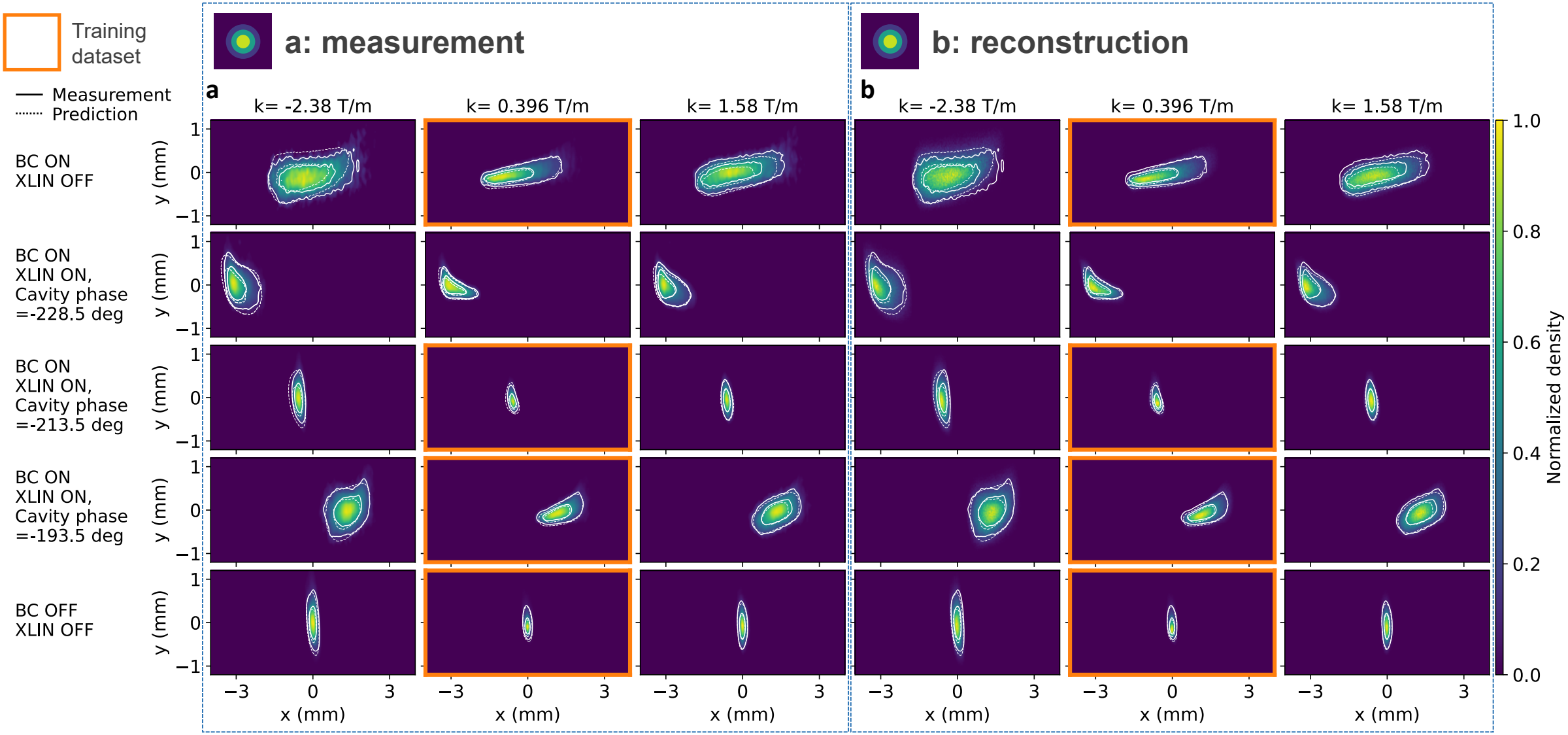

GPSR validation using downstream measurements

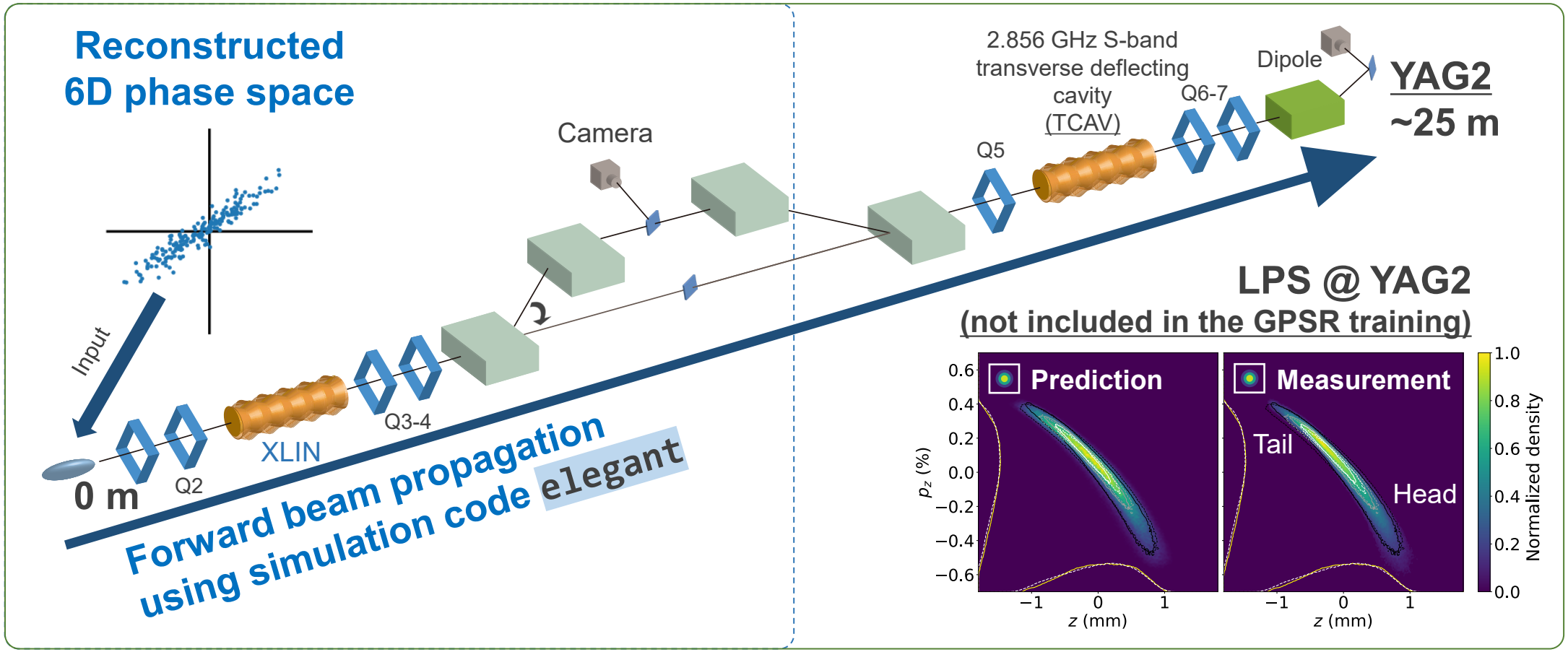

6D reconstructed phase space of the beam:

➡ **Can be used to predict the phase space at downstream beamline**

Predictions using reconstructed phase space @ YAG2

Beam image:
Measurement

Measurements
Predictions

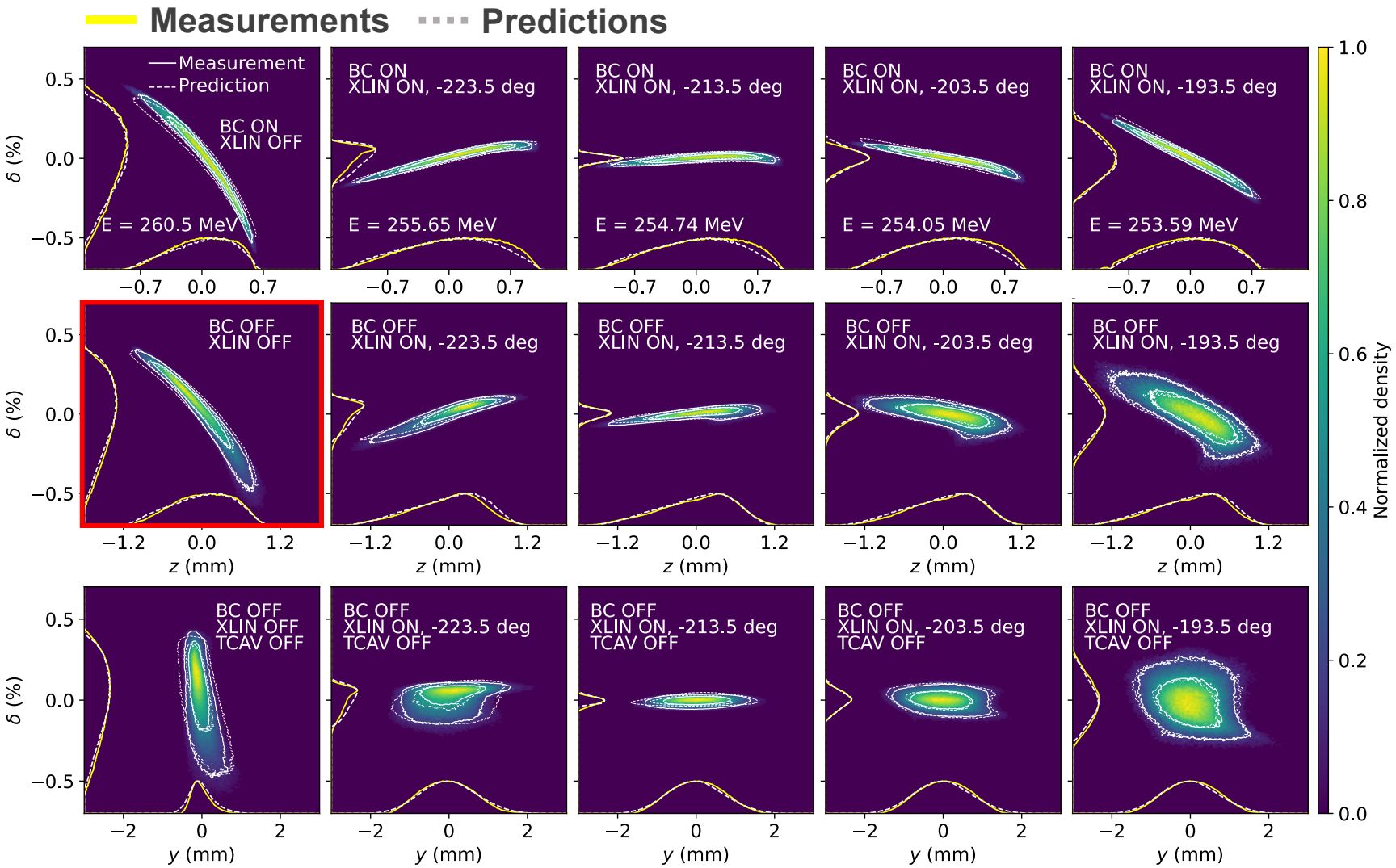

GPSR also successfully predicts independent downstream measurements!

Reconstructed phase space @ Q1 entrance

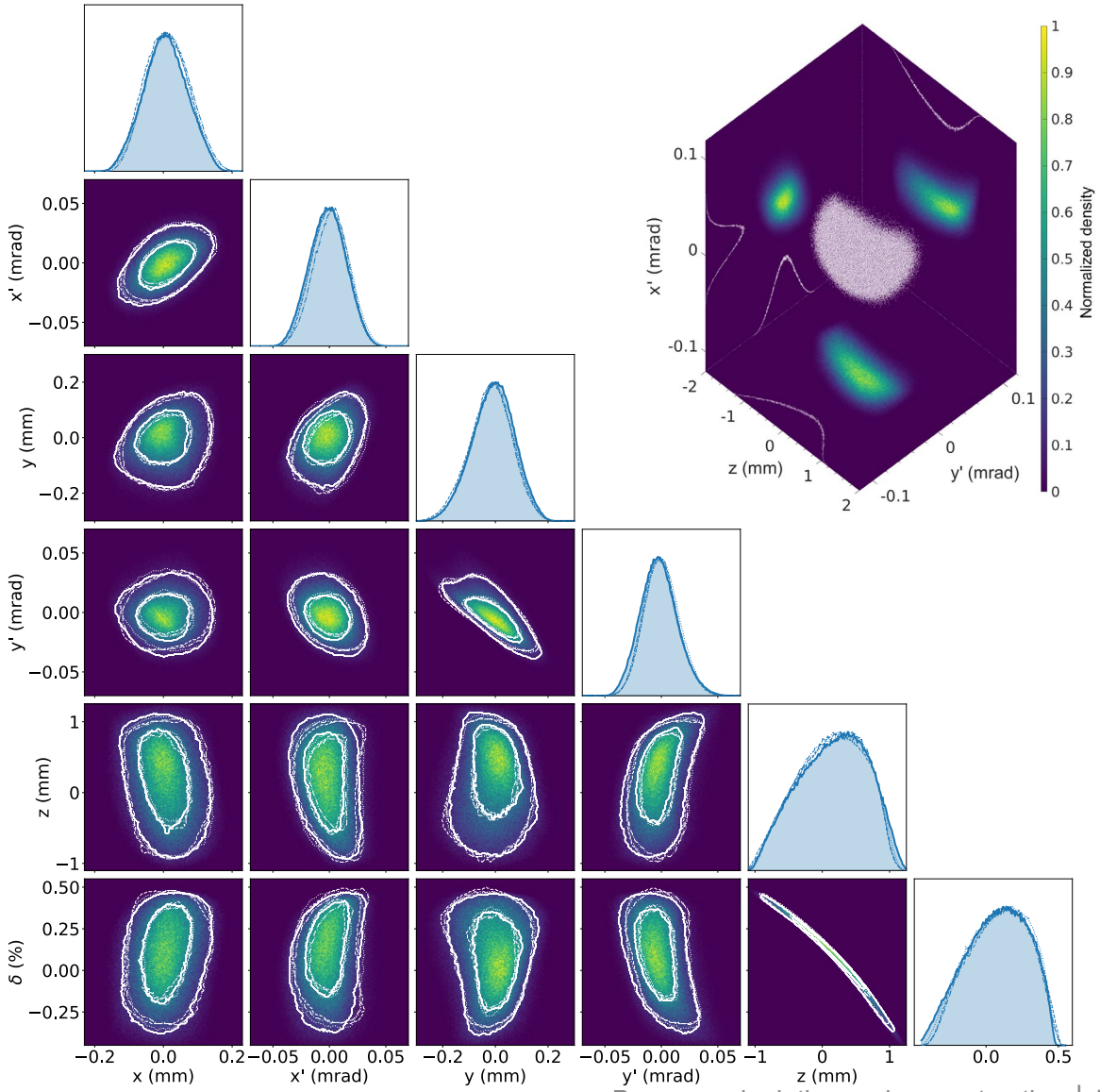

Parameters	4D Reconstruction	6D reconstruction
β_x (m)	4.59±0.08	4.51±0.07
β_y (m)	7.65±0.11	7.81±0.10
α_x (rad)	−0.55±0.02	−0.52±0.05
α_y (rad)	1.18±0.02	1.15±0.06
ε_{nx} (mm mrad)	0.43±0.01	0.43±0.01
ε_{ny} (mm mrad)	0.41±0.01	0.41±0.02

Parameters	Measurement	6D reconstruction
ε_{nz} (mm mrad)	137.34±17.240	143.36±3.87
σ_z (mm)	0.45±0.01	0.46±0.00
σ_δ (%)	0.24±0.01	0.22±0.00
Slice σ_δ(%)		0.01 (typical)

More information from 6D GPSR

- March 2026 measurement, preliminary analysis

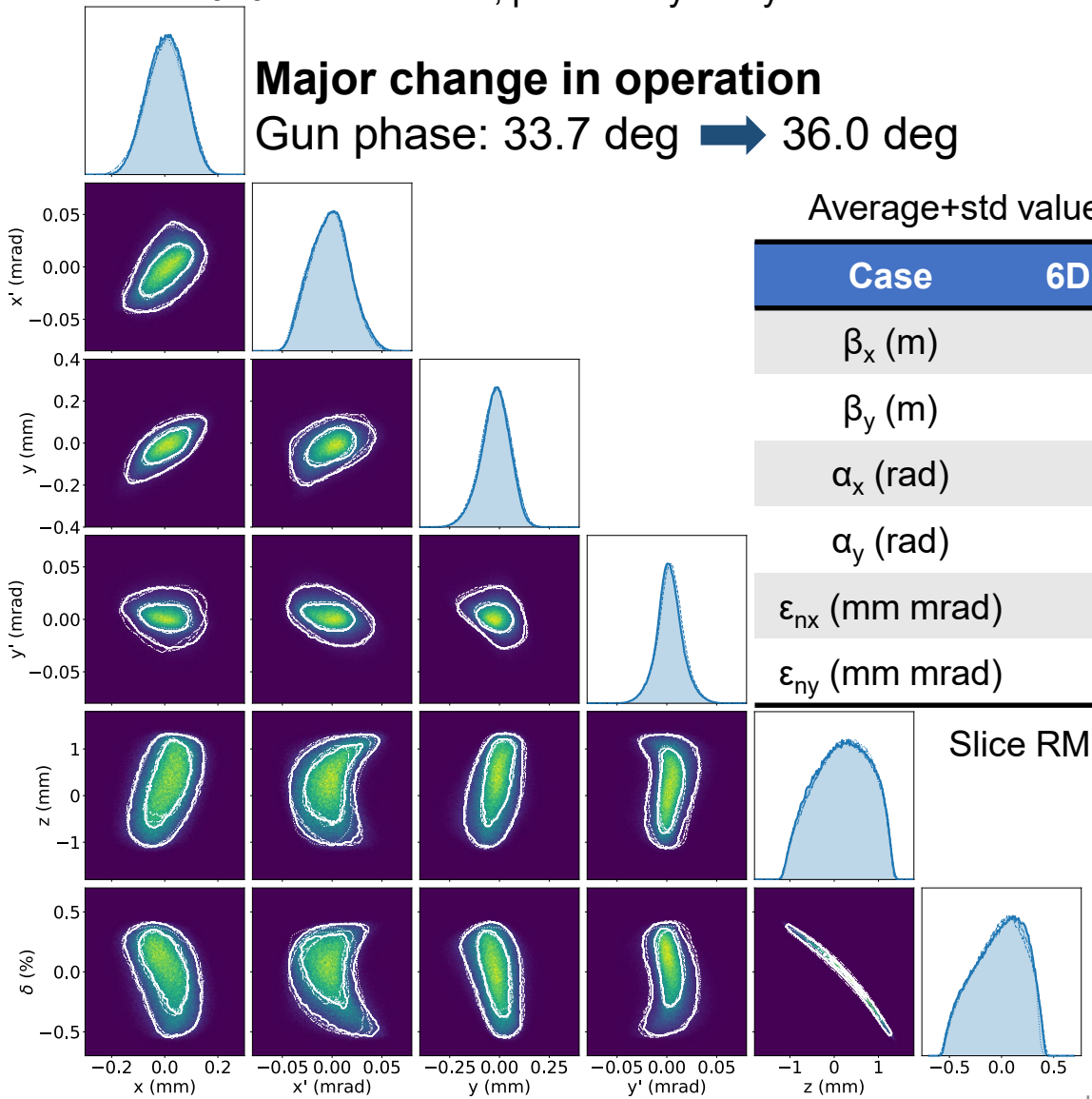

Major change in operation

Gun phase: 33.7 deg ➡ 36.0 deg

Average+std value from 15 iterations

Case	6D reconstruction
β_x (m)	4.28±0.19
β_y (m)	5.96±0.18
α_x (rad)	-0.60±0.03
α_y (rad)	0.37±0.03
ε_{nx} (mm mrad)	0.57±0.011
ε_{ny} (mm mrad)	0.45±0.013

Slice RMS energy spread: 0.01%

Longitudinal phase space: **(x,y) projection**

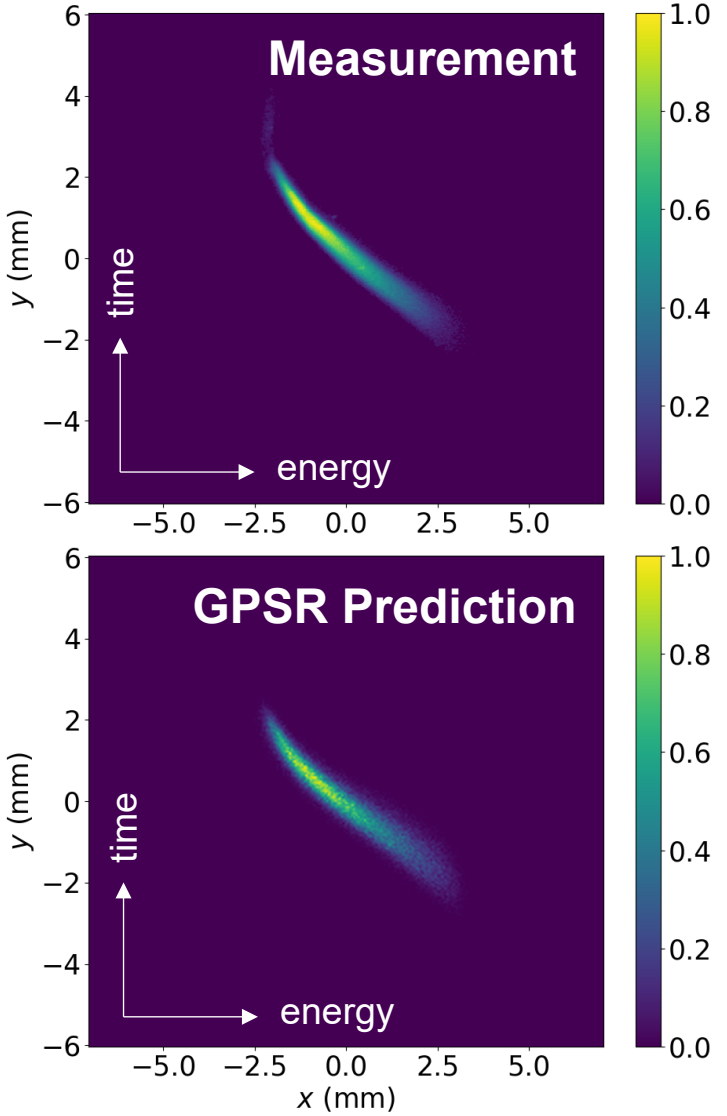

More information from 6D GPSR: x/y slice emittances

- March 2026 measurement, preliminary analysis

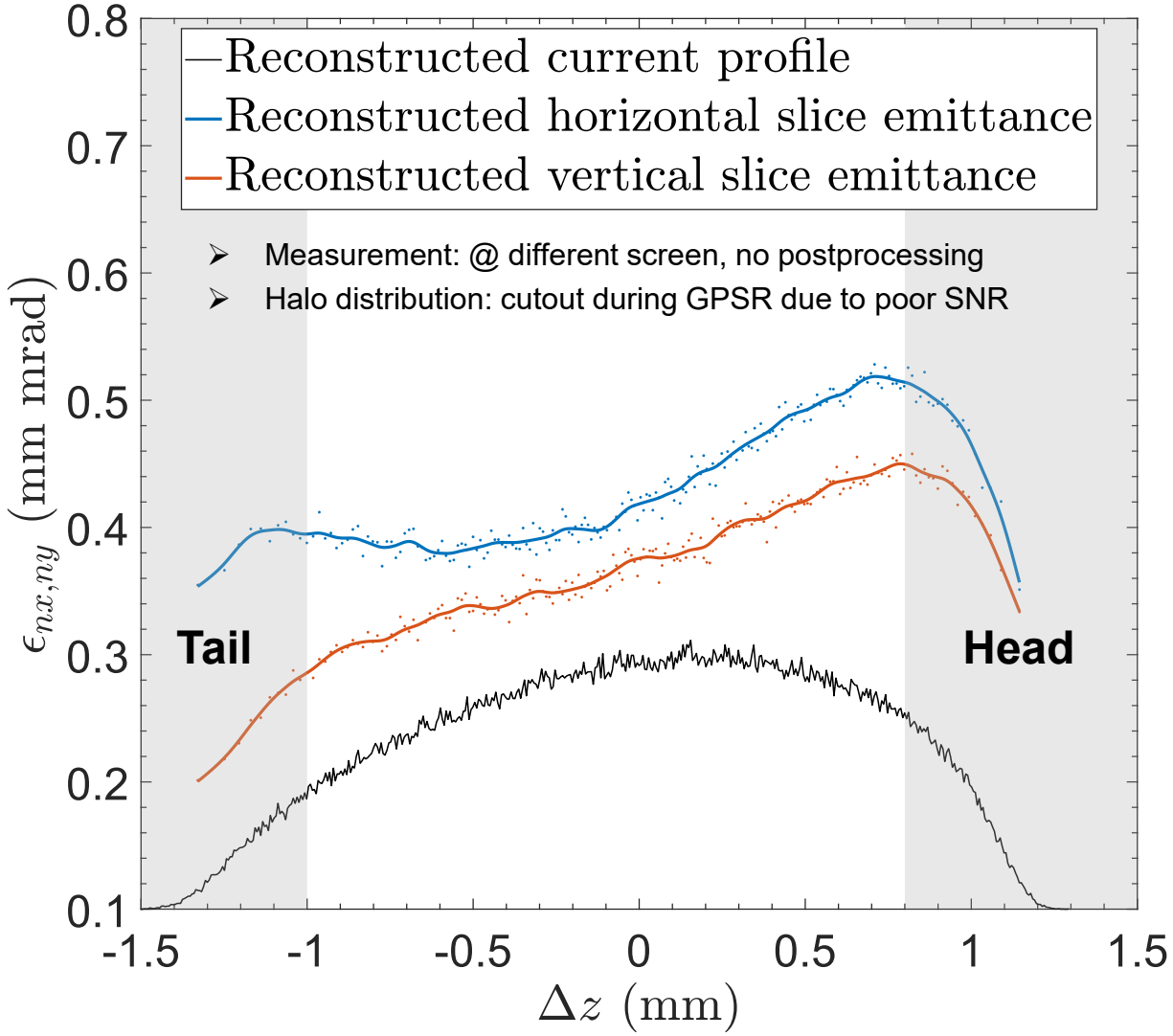

Conventional slice emittance measurement @ different screen (using TCAV)

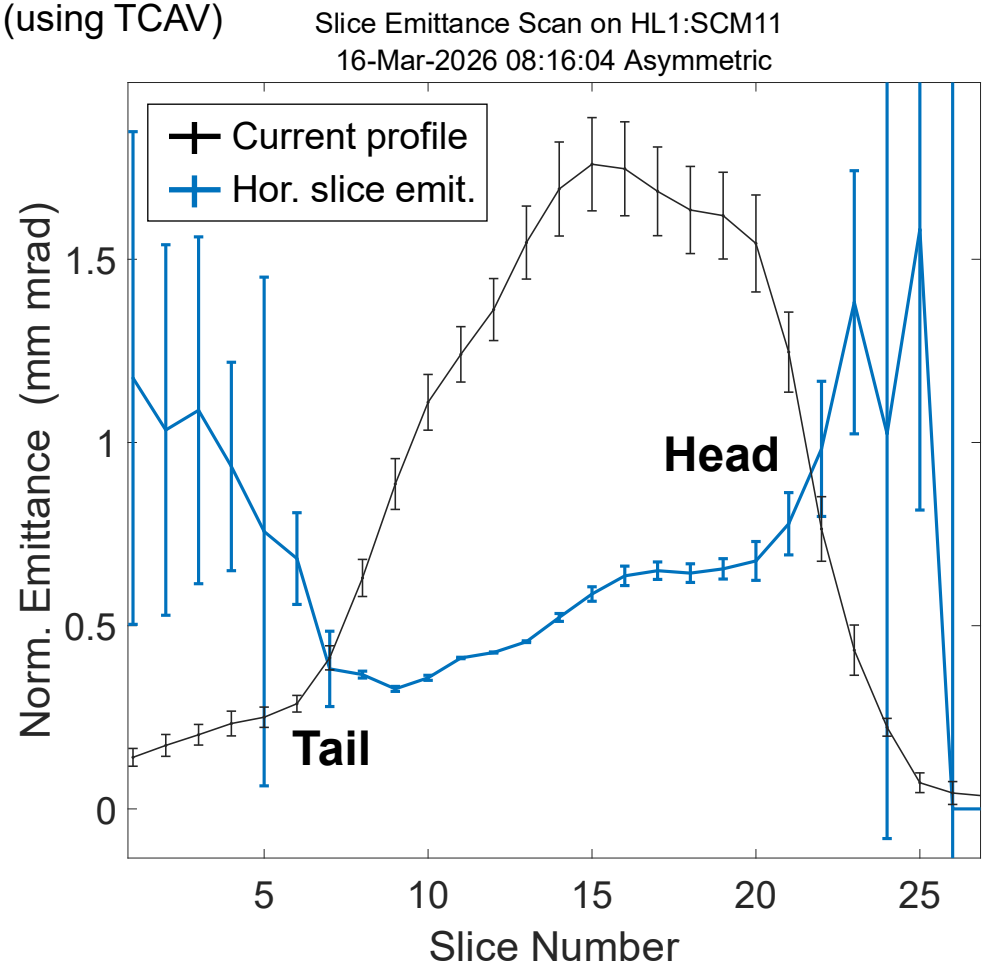

*Diagonal terms are naturally 1.0

More information from 6D GPSR: dispersion, correlations

- March 2026 measurement, preliminary analysis

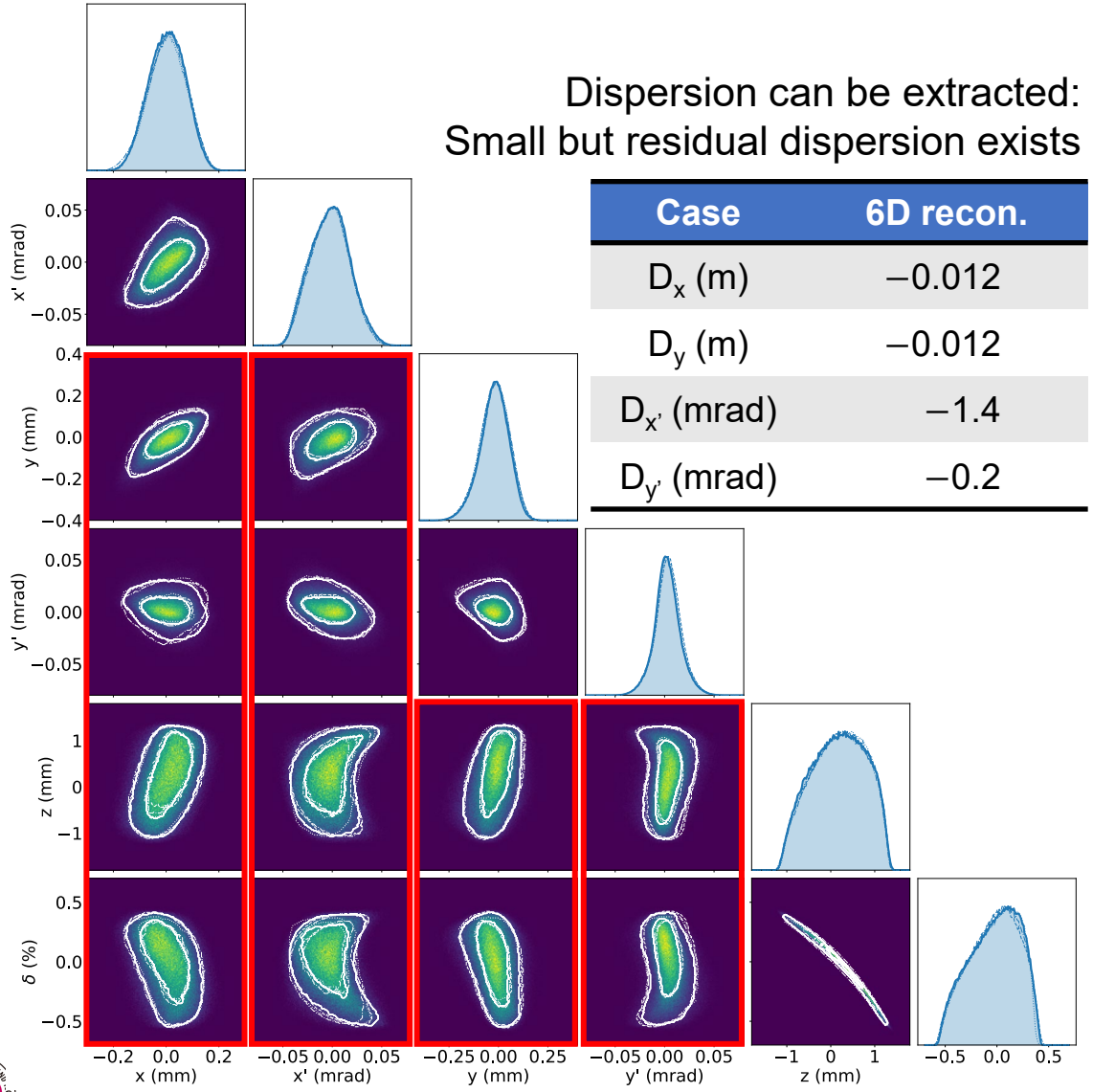

Dispersion can be extracted:
Small but residual dispersion exists

Case	6D recon.
D_x (m)	−0.012
D_y (m)	−0.012
$D_{x'}$ (mrad)	−1.4
$D_{y'}$ (mrad)	−0.2

For $\mathbf{X} = (x, x', y, y', z, \delta)$,

Pearson correlation coefficient: $\rho(i,j) = \dfrac{< X_i X_j >}{\sqrt{< X_i^2 >< X_j^2 >}}$

Coefficient close to ± 1: strongly correlated*

Coefficient for reconstructed phase space

$$\rho_{\mathbf{X}} = \begin{bmatrix} 1.000 & 0.516 & 0.673 & -0.089 & 0.425 & -0.400 \\ 0.516 & 1.000 & 0.455 & -0.430 & 0.152 & -0.174 \\ 0.673 & 0.455 & 1.000 & -0.351 & 0.378 & -0.365 \\ -0.089 & -0.430 & -0.351 & 1.000 & 0.061 & -0.029 \\ 0.425 & 0.152 & 0.378 & 0.061 & 1.000 & -0.988 \\ -0.400 & -0.174 & -0.365 & -0.029 & -0.988 & 1.000 \end{bmatrix}$$

For ideal impact+elegant simulations, correlations are typically in the order of 0.001

This information from the GPSR can be used for the optimization of beam correlations

POHANG ACCELERATOR LABORATORY

*Model calibration: currently under investigation at the PAL-XFEL
For more information on the optimization: S. Kim *et al., In. Proc. ICALEPCS 2025*, Chicago, IL, USA, **MOCG004 (2025)

Applications using 6D GPSR: beamline optimizations

- elegant simulation used

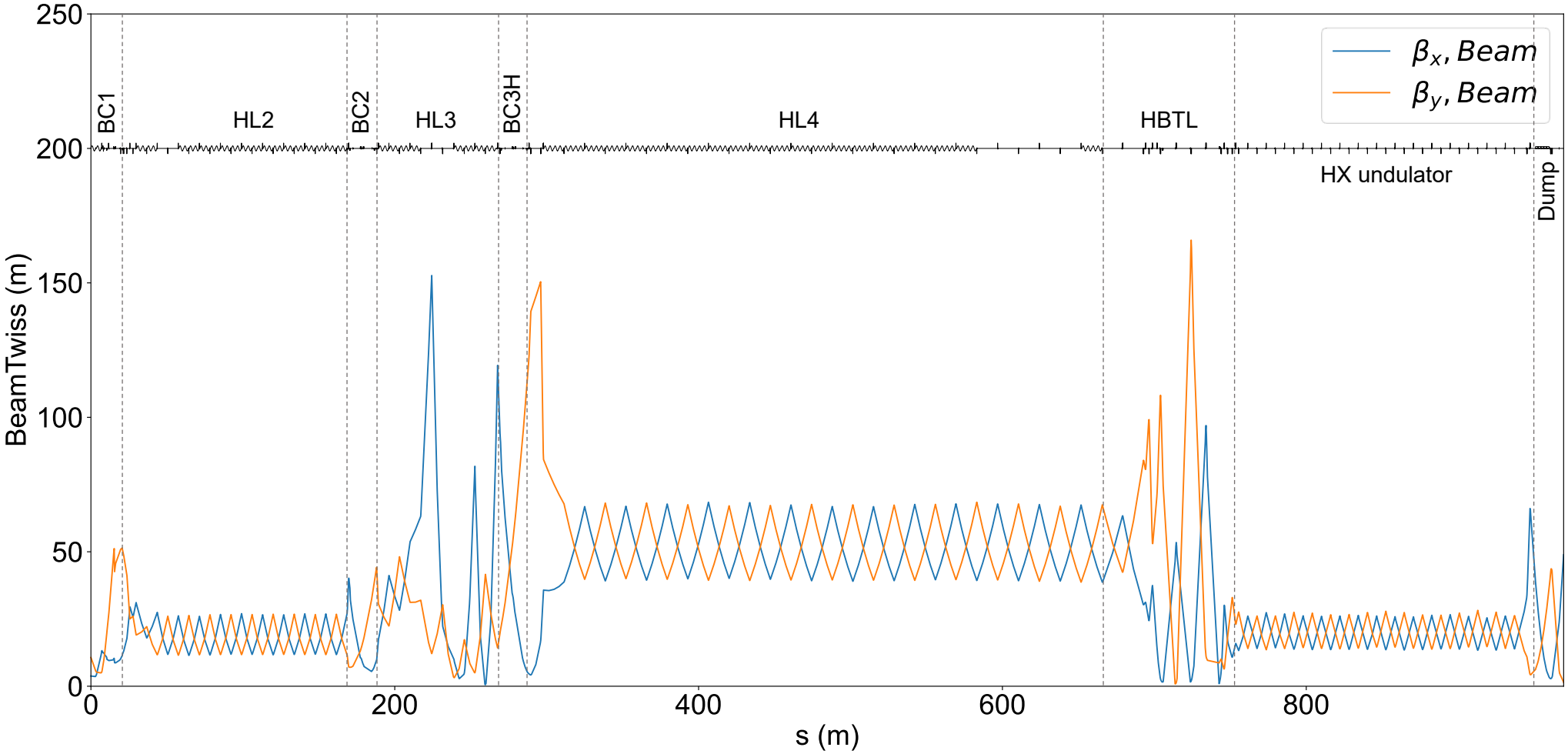

GPSR-based beam diagnostics → **optimization** → **calibrated model-based digital twin***

Summary and future works

- **Beam manipulation becomes gradually important**
  - Manipulation of cross-plane correlation, nonlinear chirp and double horn, final focus with certain shape, for high-energy physics applications and high-brightness X-ray light

- **GPSR-based phase space reconstruction was successfully demonstrated both at test and user facilities**
  - All the coupled phase spaces can be successfully predicted also for special beams
  - readily applicable using common elements such as RF cavity, quad, dipole, and screen
  - Near unique solution: can represent the physical ground truth
  - Optimization of the beamline using 6D GPSR results, incorporated into physics simulations

- **PAL-XFEL enhancement will be carried out**
  - Beam diagnostics using the GPSR technique will be performed @ PAL-XFEL to investigate the machine condition: measurement-based model calibration can be performed
  - Therefore, measurement-based optimization using calibrated model can be performed to maximize the FEL quality and on-line virtual diagnostics

Acknowledgements

PAL 포항가속기연구소 POHANG ACCELERATOR LABORATORY

POSTECH

Haeryong Yang **Seongyeol Kim** **Gyujin Kim**
Myung-Hoon Cho Chi Hyun Shim Chang-Kyu Sung
Kookjin Moon Hoon Heo

SLAC NATIONAL ACCELERATOR LABORATORY

Auralee Edelen
Ryan Roussel

We also thank the PAL-XFEL accelerator control team members and Prof. Moses Chung of POSTECH

THE UNIVERSITY OF CHICAGO

Juan Pablo Gonzalez-Aguilera (now @ SLAC)
Young-Kee Kim

Argonne NATIONAL LABORATORY

John Power Scott Doran Gongxiaohui Chen
Philippe Piot (previously @ NIU) Wanming Liu Eric Wisniewski Charles Whiteford

- This work was supported by the National Research Foundation of Korea (NRF) grant (2019R1I1A1A01041573, RS-2024-00347026, RS-2024-00455499), funded by the Korea government (MSIT).
- This work was also supported by the U.S. Department of Energy, Office of Science under Contract No. DE-AC02-06CH11357 and No. DE-AC02-76SF00515 and the Center for Bright Beams, NSF award PHY-1549132.
- This research used resources of the National Energy Research Scientific Computing Center (NERSC), a U.S. Department of Energy Office of Science User Facility located at Lawrence Berkeley National Laboratory, operated under Contract No. DE-AC02-05CH11231 using NERSC award BES-ERCAP0020725.

Pohang Accelerator Laboratory

80 Jigokro-127-beongil,
Nam-gu, Pohang,
Gyeongbuk 37673, Republic of Korea

Email: sykim12@postech.ac.kr